AD-A248 033

US Army Corps
of Engineers

PASSIVE ACOUSTIC RANGE ESTIMATION
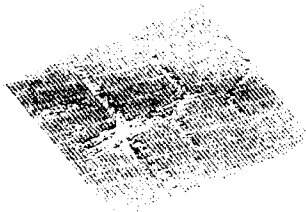# OF HELICOPTERS

by

Reo Olson, Daniel H. Cress

Environmental Laboratory

DEPARTMENT OF THE ARMY
Waterways Experiment Station, Corps of Engineers
3909 Halls Ferry Road, Vicksburg, Mississippi 39180-6199

DTIC
ELECTE
MAR 30 1992
S B D

February 1992
Final Report

92-07953

92 3 30 060

REPORT DOCUMENTATION PAGE

1. AGENCY USE ONLY (Leave blank)	2. REPORT DATE	3. REPORT TYPE AND DATES COVERED
	February 1992	Final report

4. TITLE AND SUBTITLE

Passive Acoustic Range Estimation of Helicopters

6. AUTHOR(S)

Reo Olson, Daniel H. Cress

5. FUNDING NUMBERS

US Army Project
No. 4A762719AT40
WU No. MU-001

7. PERFORMING ORGANIZATION NAME(S) AND ADDRESS(ES)

USAE Waterways Experiment Station
Environmental Laboratory
3909 Halls Ferry Road, Vicksburg, MS 39180-6199

8. PERFORMING ORGANIZATION REPORT NUMBER

Technical Report EL-92-13

9. SPONSORING / MONITORING AGENCY NAME(S) AND ADDRESS(ES)

US Army Corps of Engineers
Washington, DC 20314-1000

10. SPONSORING / MONITORING AGENCY REPORT NUMBER

11. SUPPLEMENTARY NOTES

Available from National Technical Information Service, 5285 Port Royal Road, Springfield, VA 22161

12a. DISTRIBUTION / AVAILABILITY STATEMENT

Approved for public release; distribution is unlimited

12b. DISTRIBUTION CODE

13. ABSTRACT (Maximum 200 words)

A passive acoustic method is presented that determines the velocity of a moving helicopter and its range at the closest point of approach. This method requires only the use of a single microphone if the fundamental blade rotation frequency of the helicopter is known, or two spatially separated microphones if it is not. The blade rotation frequency is generally adequately known after the helicopter is correctly classified using acoustic signature characteristics other than those discussed herein. The range estimate is considered valid for ranges of a few hundred meters with the attendant assumptions that: (a) the helicopter is traveling in a straight line, (b) the helicopter is moving at a constant velocity, and (c) the main rotor of the helicopter has a stable revolution rate typical of present operational helicopters. The technique was successfully tested on an example helicopter.

14. SUBJECT TERMS

See reverse

15. NUMBER OF PAGES

80

16. PRICE CODE

17. SECURITY CLASSIFICATION OF REPORT	18. SECURITY CLASSIFICATION OF THIS PAGE	19. SECURITY CLASSIFICATION OF ABSTRACT	20. LIMITATION OF ABSTRACT
UNCLASSIFIED	UNCLASSIFIED		

14. (Concluded).

Doppler shift
Helicopters
High-resolution frequency estimation
Passive techniques

Range estimation
Single acoustic sensor
Temporal coherence
Velocity estimation

Contents

Preface

This report should be cited as follows:

Olson, Reo, and Cress, Daniel H. Passive acoustic range estimation of helicopters. Technical Report EL-92-13, Vicksburg, MS: U.S. Army Engineer Waterways Experiment Station.

Conversion Factors, Non-SI to SI Units of Measurement

Non-SI units of measurement used in this report can be converted to SI units as follows:

Multiply	By	To Obtain
degrees (angle)	0.01745329	radians

1 Introduction

Background

Passive classification and location of military targets have significant advantages, when compared to active methods such as radars, provided passive techniques can achieve acceptable results. Active signal techniques are vulnerable to interception, "jamming," as well as location and destruction of the transmitter site. Furthermore, the creation of an energy field requires auxiliary power and other associated complexities. In contrast, passive systems sense only that energy generated by the source itself (e.g., sound, heat) or by the natural environment (e.g., light) such that monitoring of a target may go undetected. Acoustic techniques have advantages over other techniques, such as radars, when terrain or foliage masking degrades line-of-sight performance.

Helicopters represent a very significant threat to ground forces. Missions can be conducted at a low altitude where radar systems are ineffective. However, helicopter operations are particularly vulnerable to detection and potential mine activation, since they are often restricted to takeoff/landing zones and low altitude avenues of approach.

Purpose

The purposes of the study[1] presented herein are as follows:

a. To present a method, using a single acoustic sensor, for

(1) Velocity determination of approaching helicopters.

---

[1] This report is an expansion of a presentation to a NATO Conference in 1990 (Olson and Cress 1990).

(2) Expected range at the closest point of approach (CPA).[1]

b. To expand the characterization of helicopter signatures.

Approach

The approach given here exploits the repetitive nature of the helicopter signature and uses reasonable assumptions concerning the flight profile to estimate range from a single sensor. The technique uses commonly available signal processing software and hardware, such as the Fast Fourier Transform (FFT), to extract the critical information.

The approach is based on the fact that any acoustic source moving in a straight line displays the typical Doppler shift of sound waves. Figure 1 simulates the frequency of the main rotor blades of a helicopter moving at 33.5 m/sec and at an offset range of 182 m as it passes by an acoustic receiver. As will be illustrated in Chapter 2, the frequency of the approaching helicopter indicates its velocity. Moreover, the slope of the Doppler-shifted frequency illustrated in Figure 1 near CPA can be used to estimate the range.

The phenomenon that permits significant improvement in the calculation accuracy is that of temporal coherence — some sources output a very coherent (*consistent or unchanging*) basic frequency[2] over a long period of time. Evidence indicates that helicopter signals have long periods of temporal coherence (Cress and Olson 1990). Changes of the phase through time will be analyzed in later sections and used to predict the instantaneous or short-term frequency to a high degree of accuracy. When applied to real field data this approach can be used to determine the fundamental frequency, velocity, and range at CPA.

Method

The analysis of the change of the phase through time, which will be described herein, can be implemented using conventional methods and hardware,

---

[1] For convenience, symbols and abbreviations are listed in the Notation (Appendix D).

[2] The phrase "basic frequency" means the frequency without any Doppler shift. This could be any distinct band of energy (e.g., fundamental frequency of main rotor blades, second harmonic of main rotor blades, fundamental of tail rotor blades, etc.). The word "basic" is used rather than "fundamental" to emphasize that the technique also works on the higher harmonics. Likewise "basic" is used rather than "harmonics" to distinquish the frequency before Doppler shift from the value after shifting. (See Appendix A for technical definitions and Appendix B for clarification of these frequencies.)

but is subject to source parameters (see "Assumptions" below). For this study, helicopters with simple flight profiles are the applicable sources. A detailed description of the equipment (hardware) used in the field application is listed in Table 4.

The theoretical description of the method is presented in Chapter 2. The application of this method on the fundamental of the main rotor frequency of the moving helicopter is covered in detail in Chapters 3, 4, and 5. The application of this method on both the second harmonic of the main rotor and the fundamental of the tail rotor is briefly discussed in Appendix C.

Issues and Constraints

Assumptions

The velocity, range, and time of CPA can be derived from one or two receivers under certain assumptions:

a. The helicopter is traveling in a straight line.

b. The helicopter is traveling at a constant velocity.

c. The helicopter possesses a near constant *basic frequency.*

One receiver is sufficient in some circumstances (see "Number of receivers required," page 4) when enough acoustic data are available to calculate all the information.

Data requirements

If the basic frequency of the helicopter is known from sound classification (e.g., amplitude versus frequency spectrum), the acoustic information can be processed to determine the approaching velocity long before the source reaches the receiver; the range (and time) at CPA can be estimated shortly before the helicopter reaches the receiver. This information, combined with other acoustic techniques indicating the direction from which the sound is coming (Stabler, Bayiot, and Cress 1976; Dudgeon and Mersereau 1984; Smith 1984), allows timely location of the aircraft.

If the basic rotor frequency is not known, the entire problem can be solved by having two spatially separated acoustic receivers. The receiver nearest the approaching aircraft would then have the task of calculating the basic frequency and of transmitting this information back to the second receiver. Hence, the second receiver could calculate the range at

Number of receivers required

One receiver is sufficient under either of the following assumptions:

a. The basic rotor frequency of the helicopter is known.

b. Calculation of the range and velocity after the helicopter passes CPA is acceptable.

Computational accuracy

The formulas to calculate the velocity and basic frequency are simple. Only the knowledge of the approaching and retreating Doppler-shifted frequencies and the velocity of sound are required. The range formula also requires the slope of the frequency at CPA. All of these formulas can be easily derived; however, they are very sensitive to errors in the Doppler-shifted frequencies.

The primary shortcoming in using Fourier Transform methods is the accurate calculation of the required frequencies. To obtain adequate resolution of frequency for the application presented herein, conventional FFT techniques would require observation of the signature over an unacceptably long time interval. The time interval is unacceptable because the frequency is constantly changing. Since the source of the acoustic signal in this investigation is moving, frequencies detected by a non-moving receiver are changing with time (i.e., a Doppler shift occurs (Weidner and Sells 1965)). Such a shift in the frequencies causes a smearing by the FFT of the power into a number of different frequency bins,[1] decreasing the accuracy for conventional calculations. Such smearing is unacceptable for this implementation.

Recording accuracy

The addition of some noise onto the recorded signal impairs an accurate calculation of the frequency at any time using the standard FFT techniques. Wind can be a major source of noise and Doppler smearing by moving media. The presence of wind may introduce two impediments: a deterioration of the signal-to-noise ratio and changes in the travel time and frequency (Doppler shift) of the sound. These complications are not considered in this report. A poor signal-to-noise ratio is not expected to be a serious problem for ranges less than 500 m. However, the wind effect

---

[1] The concept of "frequency bins" is the discrete frequency classification that the FFT assigns to a real signal. For example, a 1-sec-long, 19.1-Hz signal would have most of its energy assigned to the 19-Hz FFT bin with the second-largest amount of energy assigned to the 20-Hz FFT bin.

on acoustic velocity could be a problem, particularly when the wind speed is greater than 10 percent of the aircraft velocity.

Potential Applications

Potential applications include reconnaissance sensors assigned to perform early detection and analysis of a helicopter acoustic signal. Another use would be for sensors assigned the decision of whether or not to activate mines. Potential locations include situating the sensors in a valley that serves as a natural avenue of approach below radar or near likely landing zones.

2 Analytical Method

The mathematical foundation for the detailed analysis includes an elementary review of the Doppler shift theory of acoustic waves. The formulas (and also the time when enough acoustic data has been collected to perform the necessary calculations) depend on whether or not the type of helicopter (and its attendant acoustic signal) is known. Both cases require an accurate knowledge of the Doppler-shifted frequencies.

To obtain the high degree of accuracy in the frequency estimate, this approach exploits conventional signal-processing theory. A close investigation of the phase information derived by the FFT of a constant-frequency wave provides the basis for the significantly improved accuracy.

Doppler Theory

The most general case, the non-recognized helicopter, requires very little knowledge of the approaching target. Two spatially separated receivers are suited for this situation. Other alternatives are use of a single receiver with correct classification of the helicopter using the acoustic signature or use of a supplemental sensor, such as a thermal infrared (IR) radiometer and determination of the acoustic fundamental from the modulation of the blade rotation. If two receivers are used, the front receiver has the task of calculating the basic frequency of the helicopter and relaying it to the second acoustic receiver for additional calculations. Both receivers may also be able to independently calculate the velocity, range at CPA, and time of CPA. For the approach presented herein, the front receiver will not be able to calculate this information until after the helicopter has passed. The second receiver, in the unknown helicopter case, can calculate this information just before the helicopter reaches CPA. This second receiver can then be programmed for the case where the type of helicopter is known and only one microphone is required. Hence, only one receiver will be considered here.

Assumptions

Table 1 summarizes the assumptions required for the following calculations. The principal reason for assuming only one moving source is to ensure the possibility of separating the signals in the frequency domain. Extension to multiple sources at the same acoustic generation frequencies will require further study. This separation is needed to accurately determine the approaching and retreating far-field frequencies and the slope of the frequency near CPA. The second assumption of a constant velocity and direction is probably not valid over long periods of time but is applicable for short intervals. An analysis of the data can usually determine whether this assumption is valid.

Table 1 Assumptions for One Acoustic Receiver
■ There is only one moving noise source.
■ The helicopter is traveling at a constant velocity (V) in a straight line.
■ The velocity of sound (C) from the helicopter to the receiver is constant and is known.
■ V is less than C.
■ The helicopter outputs a basic frequency (f_0) that remains constant when measured by an observer in the helicopter (i.e., the helicopter point of view).

The last assumption in Table 1 implies that any frequency change measured at a fixed receiver is caused by a Doppler shift. The validity of this assumption for a Chinook helicopter (CH-46) was one of the main conclusions of Cress and Olson (1990): that the source emits a temporally coherent signal at the fundamental over time periods on the order of 15 sec.

Calculations

Figure 2 is derived from a model subject to the assumptions in Table 1. In this application, the term "far field" means that the separation between the source and the receiver is enough to ensure that the Doppler-shifted frequency is less than 10 percent of the total change of the Doppler shift for the approaching frequencies relative to the retreating frequencies. In both cases the receiver records a signal with essentially a constant frequency. Standard Doppler theory yields the following formulas:

$$f_a = \frac{f_o}{1 - \dfrac{V}{C}} \tag{1}$$

$$f_r = \frac{f_o}{1 + \dfrac{V}{C}} \tag{2}$$

where

f_a = the approaching frequency

f_o = basic acoustic frequency of the source

V = velocity of that source

C = velocity of sound in still air

f_r = retreating frequency

These two formulas can be solved for f_o and V in terms of f_a, f_r, and C:

$$f_o = \frac{2 f_a f_r}{f_a + f_r} \tag{3}$$

$$V = C \cdot \frac{f_a - f_r}{f_a + f_r} \tag{4}$$

The aircraft at CPA is sending out a signal to the receiver at frequency f_o. A more involved calculation subjected to the assumption in Table 1 shows that when the helicopter passes the receiver at a range R at CPA, the slope of the change in the frequency f at CPA determines the range (R):

$$R = \frac{- f_o \cdot V^2}{C \cdot \frac{df}{dt} (CPA)} \tag{5}$$

Time delay from aircraft to receiver

The time required for sound to travel from the helicopter to the receiver actually introduces a slight change in the shift of the frequencies. However, this shift has no impact on the far-field approaching and retreating frequencies, and minimal impact on the slope of the Doppler shift at CPA. This difference is illustrated in Figure 3 for the situation shown in the acoustic plot of Figure 1. Consequently, the time shift will be ignored in the derivation.

Calculations when the basic frequency is known

As soon as the far-field approaching frequency f_a is detected and analyzed, the approaching velocity V can be calculated with the following formula:

$$V = C \cdot \frac{f_a - f_o}{f_a} \qquad (6)$$

This formula is derived from Equation 1. The formula for the range at CPA remains unchanged from Equation 5 and is repeated below:

$$R = \frac{-f_o \cdot V^2}{C \cdot \frac{df}{dt}(CPA)} \qquad (5)$$

Time of CPA

It should be noted that when the aircraft is at CPA, it is sending a frequency to the receiver that is not frequency shifted. If t_o represents the time at which the ground is receiving a Doppler-shifted frequency $f(t_o)$, and if $f(t_o)$ equals f_o, then the sound was generated when the aircraft was at CPA. Since that sound travels a distance R at a velocity C, the actual time the aircraft was at CPA (t_{CPA}) is

$$t_{CPA} = t_o - \left(\frac{R}{C}\right) \qquad (7)$$

If the slope of the frequency remains approximately constant for some time before CPA, the actual time and range at CPA of the aircraft can be estimated before it reaches that point using the slope from the earlier times (t):

$$R(t) = \frac{-f_o \cdot V^2}{C \cdot \frac{df}{dt}(t)} \qquad (8)$$

The slope of the line tangent to the current frequency curve at a time t before CPA can also be used to estimate the slope between the current point $(t, f(t))$ on the curve and the point (t_o, f_o) of CPA (see Figure 4):

$$\frac{df}{dt}(t) \approx \frac{f_o - f(t)}{t_o - t} \qquad (9)$$

Solving Equation 9 for t_o yields the estimate $t_o(t)$ (made at time t) of when the sound made at CPA will reach the receiver

$$t_o(t) = t + \frac{f_o - f(t)}{\frac{df}{dt}(t)} \qquad (10)$$

Using this value and Equation 8 in the formula for the actual time that the aircraft is at CPA, Equation 7, yields the estimate at time t of the time of CPA

$$t_{CPA}(t) = t + \frac{f_o - f(t)}{\frac{df}{dt}(t)} - \frac{-f_o \cdot V^2}{C^2 \cdot \frac{df}{dt}(t)}$$

which can be simplified to

$$t_{CPA}(t) = t + \frac{[f_o - f(t)] \cdot C^2 + f_o \cdot V^2}{C^2 \cdot \frac{df}{dt}(t)} \tag{11}$$

This equation is the one of interest if the intention is to intercept the aircraft. It represents the estimate (made at a time t) of when the aircraft will actually arrive at CPA. The key assumption of this formula is that the slope of the frequency curve approximates the corresponding slope when the aircraft is at CPA. The expected range is given in Equation 8.

Accurate Calculation of Frequency

The previous formulas are of limited value if the frequency is not known accurately. The standard FFT calculation over an interval of time has a relationship that limits the resolution of the frequency:

$$1 = [Frequency\ Increment\ (Hz)] \cdot [Time\ Interval\ Length\ (sec)] \tag{12}$$

This formula suggests that resolving a signal to within 0.1 Hz requires applying the FFT to a 10-sec-long signal. This may be possible in the far-field situation, but it is definitely not applicable near CPA for a moving helicopter on the order of 30 m/sec or greater at ranges of several hundred meters or less. Near CPA the required accuracy on the frequency is much higher since the slope of the frequency must be precisely calculated to determine the range (Equation 8) and time of CPA (Equation 11). Unfortunately, near CPA the frequency of the signal is changing rapidly; thus, the FFT of a long time interval will represent only an average of that time interval and will definitely not represent an estimate of the instantaneous frequency required for the above formulas.

Selection of a short time interval for the FFT results in poor resolution of the frequency if the conventional calculations are assumed (see Figure 5). If the time interval is only 0.5 sec in length, the resolution of the frequency provided by the FFT is only 2 Hz. It should be noted that the entire Doppler shift of the strongest signal (Figure 1) is less than 5 Hz. Clearly, a 2-Hz resolution of the frequency is useless for calculating the slope at CPA for that signal.

An improved frequency resolution can be obtained with the concepts of the temporal coherence of the source signal and a careful analysis of the phase of the cross-spectral density (CSD). A simple example illustrates these concepts. The method exploits the assumption that the bandwidth of the unknown source basic frequency is significantly narrower than the frequency lines in the FFT.

Examination of the FFT

FFT of a 19.1-Hz signal. Suppose the FFT was used to analyze a signal $h(t)$ which is actually a pure 19.1-Hz cosine wave:

$$h(t) = \cos(2\pi \cdot 19.1 \cdot t)$$

Assume that successive 1-sec intervals will be used to analyze this signal. According to Equation 12, this interval length permits a 1-Hz frequency resolution. Consider the 19-Hz term of the FFT. The FFT will identify two real numbers A and θ for which the function $g(t)$ closely matches $h(t)$.

$$g(t) = A \cos(2\pi \cdot 19 \cdot t + \theta)$$

Significance of phase term. Clearly the amplitude A should be approximately 1, but θ will definitely depend on the time interval [n,n+1] over which the FFT was calculated (see Figure 6). By rewriting $h(t)$ as

$$h(t) = \cos\left(2\pi \cdot 19 \cdot t + 2\pi \cdot \frac{t}{10}\right) \tag{13}$$

it seems reasonable that θ represents the average of the term $2\pi \cdot t/10$ over the time interval [n,n+1]

$$\theta(n) = \frac{\left[\dfrac{2\pi \cdot n}{10} + \dfrac{2\pi \cdot (n+1)}{10}\right]}{2}$$

$$\tag{14}$$

$$= \pi \cdot \frac{(2n+1)}{10}$$

Graphically this implies that the FFT frequency domain transformation of successive time intervals rotates around the origin of the complex plane at a constant rate. The first point plots at an angle of $\pi/10$ rad with respect to the positive x-axis. The succeeding points plot at $3\pi/10$, $5\pi/10$, $7\pi/10$, $9\pi/10$, $11\pi/10$, $13\pi/10$, $15\pi/10$, $17\pi/10$, $19\pi/10$, $\pi/10$, $3\pi/10$, $5\pi/10$, ... for the [n,n+1], n= 1, 2, ... time intervals. It takes 10 sec for the 19-Hz FFT frequency domain value to move around the complex unit circle (Ahlfors 1966) when analyzing the 19.1-Hz signal (see Figure 7).

Impact on the CSD

Phase changes with time. This constant phase rotation of the angles of the FFT response over succeeding time intervals indicates that the difference β in these phases remains constant. For example, for the 19.1-Hz signal, the difference between the total phase estimates for succeeding time intervals n to n+1 is given by:

$$\beta = \frac{2\pi}{10} \, rad \tag{15}$$

Now Equations 13 and 14 can be written as

$$\theta(n) = \theta(0) + n \cdot \beta \tag{16}$$

and

$$h(t) = \cos (2\pi \cdot 19 \cdot t + \beta \cdot t)$$

$$= \cos \left[2\pi \cdot \left(19 + \frac{\beta}{2\pi} \right) \cdot t \right] \tag{17}$$

This formula appears to be close to the original definition of $h(t)$ in Equation 13. However, Equation 17, which expresses a completely different point of view, states that if the phase differences of the 19-Hz FFT of successive time intervals are constantly equal to β radians, then a (19 + $\beta/2\pi$)-Hz signal might exist in the time domain.

Definition of CSD. If $H_n(f)$ is defined to be the complex number that is the output of the FFT applied to the signal $h(t)$ at f Hz of the time interval [n,n+1], then the CSD of this signal and frequency over that time interval, $X_n(f)$, is defined as

$$X_n(f) = H_n(f) \cdot \left[H_{n-1}(f) \right]^* \tag{18}$$

where the * denotes the complex conjugate. The phase of the CSD represents the difference in the phases of successive time intervals, [n-1,n] to [n,n+1], of the FFT of the frequency f. This suggests that the phase of $X_n(f)$ represents the instantaneous change of the phase of the f-Hz component of the h(t) signal at time t = n.

In the example of the signal h(t) representing the 19.1-Hz cosine wave, the CSD of 19 Hz, $X_n(19)$ has a constant phase of

$$\beta = \frac{2\pi}{10} \, radians$$

$$= 0.1 \, cycles$$

Likewise, if a pure $(19+\delta f)$-Hz signal with $|\delta f|<.5$ is transformed to the frequency domain and analyzed with the CSD of adjacent 1-sec intervals, then the phase of the 19-Hz CSD will be constant at δf cycles.

Complex plane graph over time of the CSD. Since the plot of the FFT rotates around the unit circle at constant phase increments and the CSD represents the phase difference of the FFT, logically the CSD will be a constant for the pure signal. Hence, all the CSD points, $X_n(19)$ $n=1, 2, \ldots$ of a pure $(19+\delta f)$-Hz signal in the complex plane will actually plot on top of each other δf of the way around the unit circle (see Figure 7) if the amplitude does not change with time. In the presence of a small amount of recording noise or possibly a slightly impure signal, all these points will plot in roughly the same location of the complex plane.

Cumulative sum of the CSD. In the presence of moderate noise, the CSD signal would plot over a much larger range of angles in the complex plane. One way to determine the overall trend is to use complex addition over N+1 adjacent time intervals to add the signal and cancel the noise:

$$\sum_{n=1}^{N} X_n(f) = \sum_{n=1}^{N} H_n(f) \cdot [H_{n-1}(f)]^* \tag{19}$$

The plot of the cumulative sum of the CSD (Figure 8) will clearly show a trend for a narrow band frequency input with a good signal-to-noise ratio. Successive points should plot in roughly a straight line radiating away from the origin (Figure 8). That figure plots the locations of the sum for N=1, 2, . . . 14.

Important inverse problem. Up to this point the frequency content of the time signal was usually known. Suppose the current task was to analyze the frequency content of an unknown signal h(t). If the FFT is calculated for two successive time intervals [n-1,n] and [n,n+1] and the largest amplitude stays at 19 Hz, can a better estimate of the frequency be made?

The above calculations indicate that, when measured in cycles, the phase of the CSD of the 19-Hz frequency between these two adjacent time intervals is really the difference between the actual frequency content of the signal (measured in Hz) and 19 Hz:

If 19 Hz is the largest CSD amplitude of a real signal, then

$$Actual\ Frequency\,(Hz)\ =\ 19\,Hz\ +\ \frac{CSD\ Phase\ of\ 19\ Hz\,(cycles)}{Length\ of\ FFT\ Interval\,(sec)} \tag{20}$$

where the phase of the CSD is between -.5 and .5.

For a signal with good signal-to-noise ratio, the above computation can be made for each successive CSD value (between each successive FFT interval). The presence of noise does degrade the estimate of the actual

frequency. Assuming that the signal is not changing significantly over time, the cumulative sum of a number of CSD values should have a phase that minimizes the corruption of the noise, yielding a better phase value than the individual CSD numbers in Equation 20.

Temporal coherence implications

The sum of the products of the FFT of a signal h(t) multiplied by the complex conjugate of the preceding interval (20) actually represents the numerator of the temporal coherence, TemCoh(f), of the signal h(t) at the frequency f

$$
TemCoh(f) = \frac{\displaystyle\sum_{n=1}^{N} H_n(f) \cdot \left[H_{n-1}(f)\right]^*}{\left[\displaystyle\sum_{n=1}^{N} |H_n(f)|^2\right]^{1/2} \cdot \left[\displaystyle\sum_{n=1}^{N} |H_{n-1}(f)|^2\right]^{1/2}} \tag{21}
$$

The previous calculations indicate that if a signal has a consistent frequency over time close to f, then the temporal coherence should have a constant phase and an amplitude close to one. In fact, that phase measured in cycles defines how much the original signal's frequency (measured in hertz) differs from f.

On the other hand, if the amplitude of the temporal coherence is not close to unity, then neither the phase of the temporal coherence nor the phase of the cumulative sum of the CSD over that long a collection of time intervals should be used as a replacement for the CSD phase in Equation 20. A plot of the graph of the cumulative sum of the CSD (e.g., Figure 9) shows good coherence when the plot radiates in approximately a straight line from the origin.

Amplitude significance

It is important to include the amplitude in the analysis along with phase and temporal coherence. The significance can be directly seen by considering the pure 19.1-Hz cosine signal again. ·

The 20-Hz FFT analysis of the 19.1-Hz signal. The same analysis can be performed on the same signal—but using the 20-Hz FFT and CSD analysis. Our time signal h(t) can be rewritten so that the 20 Hz will see it:

$$h(t) = \cos(2\pi \cdot 19.1 \cdot t)$$

(22)

$$= \cos(2\pi \cdot 20 \cdot t - 2\pi \cdot 0.9 \cdot t)$$

Hence, the FFT will see a constant phase shift of $-2\pi \cdot 0.9$ rad (or -0.9 cycles) over successive 1-sec-long intervals. Again the phase change of the FFT is the phase of the CSD. Since the CSD and FFT phases are only analyzed to within one revolution of the unit circle, this phase change of the FFT will be reported by the CSD to be $+2\pi \cdot 0.1$ rad (or $+0.1$ cycle). This value for 20 Hz is exactly the same CSD phase seen in the 19-Hz CSD analysis.

Since the CSD for 20 Hz is constant at 0.1 cycle for all 1-sec-long time intervals, the cumulative sum of all CSD values will align, and the temporal coherence will be 1.0 also. One might be tempted to claim (in the spirit of Equation 20 if the amplitude was ignored) that we are actually analyzing a pure 20.1-Hz signal. The major difference between the FFT, CSD, and cumulative sum of the CSD for 20 Hz, and their counterparts for 19 Hz, is the amplitude of all these complex numbers. The 19-Hz amplitudes will be significantly larger.

CSD phase for all frequencies. In theory, the CSD phase of our 19.1-Hz signal will be exactly the same for all 1-Hz frequency analysis values in the frequency domain (e.g., the 18-Hz and 21-Hz CSD phase will also be 0.1 cycle). Likewise the phase of the cumulative sum will always be 0.1.

The words "in theory" preface this section because, in reality, the machine significance restrictions of all computers will show some differences in the phase. The difference should increase as the analysis frequency moves away from the pure 19.1-Hz signal (see Table 2).

CSD amplitude for all frequencies. The only difference in these complex numbers is in their amplitude. The closer the analysis frequency is to 19.1 Hz, the higher the amplitude of the complex number will be. See Table 3 for a summary of the coherence amplitude (over fifteen 1-sec-long intervals) and the first few CSD amplitudes and phases for the pure 19.1-Hz cosine signal.

Amplitude of TemCoh for all frequencies. Finally, the amplitude of the temporal coherence is useless (in the case of a pure unchanging signal) for determining which analysis frequency is important. The amplitude of the coherence (the coherence column of Tables 2 and 3) is close to 1.0 for all frequencies near 19.1 Hz.

Table 2
Cross-Spectral Density Phase of a 19.1-Hz Cosine Function

Frequency (Hz)	Coherence (15 sec)	Phase (degrees) for Successive Time Intervals (sec)					
		[0,1] [1,2]	[1,2] [2,3]	[2,3] [3,4]	[3,4] [4,5]	[4,5] [5,6]	[5,6] [6,7]
10.0	0.881	25.4	52.7	55.7	26.9	19.3	25.4
11.0	0.908	27.1	50.4	52.8	28.5	21.2	27.1
12.0	0.932	28.7	48.2	50.1	30.0	23.1	28.7
13.0	0.952	30.1	46.1	47.6	31.2	24.9	30.1
14.0	0.968	31.4	44.2	45.3	32.3	26.8	31.4
15.0	0.980	32.5	42.4	43.1	33.3	28.6	32.5
16.0	0.989	33.5	40.7	41.2	34.1	30.5	33.5
17.0	0.995	34.4	39.1	39.4	34.9	32.3	34.4
18.0	0.999	35.2	37.6	37.7	35.5	34.1	35.2
19.0	1.000	35.9	36.1	36.1	36.0	35.8	35.9
20.0	0.999	36.5	34.8	34.7	36.4	37.6	36.5
21.0	0.997	37.1	33.6	33.4	36.7	39.3	37.1
22.0	0.993	37.5	32.4	32.1	37.0	41.0	37.5
23.0	0.989	37.9	31.3	30.9	37.2	42.7	37.9
24.0	0.983	38.2	30.2	29.8	37.3	44.4	38.2
25.0	0.977	38.5	29.3	28.8	37.4	46.1	38.5
26:0	0.970	38.7	28.3	27.9	37.4	47.7	38.7
27.0	0.963	38.9	27.5	27.0	37.4	49.3	38.9
28.0	0.956	39.0	26.6	26.1	37.4	50.9	39.0
29.0	0.949	39.1	25.8	25.3	37.3	52.5	39.1
30.0	0.941	39.1	25.1	24.6	37.2	54.0	39.1

Table 3
Cross-Spectral Density Amplitude of a 19.1-Hz Cosine Function

| Frequency (Hz) | Coherence (15 sec) | Time intervals (sec) Being Multiplied | | | | | |
		[0,1] [1,2]	[1,2] [2,3]	[2,3] [3,4]	[3,4] [4,5]	[4,5] [5,6]	[5,6] [6,7]
10.0	0.881	0.00014	0.00008	0.00007	0.00014	0.00019	0.00014
11.0	0.908	0.00018	0.00010	0.00010	0.00017	0.00022	0.00018
12.0	0.932	0.00022	0.00014	0.00014	0.00021	0.00027	0.00022
13.0	0.952	0.00029	0.00020	0.00020	0.00028	0.00035	0.00029
14.0	0.968	0.00041	0.00031	0.00030	0.00040	0.00047	0.00041
15.0	0.980	0.00062	0.00049	0.00049	0.00061	0.00070	0.00062
16.0	0.989	0.00106	0.00090	0.00089	0.00105	0.00116	0.00106
17.0	0.995	0.00227	0.00204	0.00203	0.00225	0.00241	0.00227
18.0	0.999	0.00814	0.00770	0.00768	0.00810	0.00839	0.00814
19.0	1.000	0.96903	0.96436	0.96407	0.96857	0.97164	0.96903
20.0	0.999	0.01179	0.01229	0.01232	0.01183	0.01151	0.01179
21.0	0.997	0.00261	0.00284	0.00286	0.00263	0.00248	0.00261
22.0	0.993	0.00110	0.00126	0.00127	0.00112	0.00102	0.00110
23.0	0.989	0.00060	0.00071	0.00072	0.00061	0.00055	0.00060
24.0	0.983	0.00038	0.00046	0.00047	0.00039	0.00033	0.00038
25.0	0.977	0.00026	0.00033	0.00033	0.00026	0.00022	0.00026
26.0	0.970	0.00019	0.00025	0.00025	0.00019	0.00016	0.00019
27.0	0.963	0.00014	0.00019	0.00020	0.00015	0.00012	0.00014
28.0	0.956	0.00011	0.00015	0.00016	0.00011	0.00009	0.00011
29.0	0.949	0.00009	0.00013	0.00013	0.00009	0.00007	0.00009
30.0	0.941	0.00007	0.00011	0.00011	0.00008	0.00006	0.00007

Analytical Summary

Using the temporal coherence and a detailed analysis of the signal phase permits a more detailed resolution of the frequency of a signal. The approach presented here and for the subsequent measured data is to perform an FFT over 1-sec-long time intervals. Next, the cross-spectral density of adjacent intervals is calculated. The signal of interest is located by choosing that integer frequency yielding the peak amplitude of the cross-spectral density. Then the phase of the CSD of that signal is used to obtain a resolution of the frequency beyond the 1-Hz limitation of the FFT. If the signal remains coherent over a length of time (as determined by the temporal coherence), the amplitude and phase of the cumulative sum of the CSD yields an improved estimate.

In theory, the resolution is infinite if the source signature is infinitely narrow. In practice, the noise on the data, the resolution of the digitizing process, the bandwidth of the source, and the computer machine significance will limit the frequency accuracy. The application of this approach to the measured acoustic data that follow shows improvement over conventional processing even with the corruption of the data by wind and a 60-Hz noise source, and with only four digits of accuracy coming from the digitizing process.

This improved resolution of a Doppler-shifting frequency permits the calculation of the basic frequency, velocity, time of CPA, and range at CPA of a source moving in a straight line (and therefore the range as a function of time). All of these data can be calculated with one receiver. The basic source frequency (i.e., not Doppler-shifted frequency) and velocity can be calculated from the knowledge of the Doppler-shifted frequencies. The range at CPA and time of CPA can be calculated from the knowledge of the basic frequency, velocity, and slope of the frequency near CPA.

If the basic frequency of the source is known a moderate time before it reaches CPA, the velocity can be calculated when the far-field approaching Doppler-shifted frequency is known. As the source approaches CPA, calculating estimated time of CPA and estimated range at CPA is possible. These estimates improve as the source approaches CPA.

3 Analysis of Far-Field Frequency for Measured Data

Statistics on Vicksburg Helicopter Test

Acoustic measurements were obtained in June 1990 by personnel of the Battlefield Environment Group, Environmental Laboratory, U.S. Army Engineer Waterways Experimental Station. The acoustic data were recorded at the Vicksburg Municipal Airport on U.S. Highway 61 south of the city of Vicksburg.

Test description

Figure 10 illustrates the field geometry of the run. All of the information presented below was gathered from one test. The statistics of Run 21 are presented in Table 4 and include data on the recording equipment, source, flight path, and weather.

As previously stated, one sensor does not permit determination of the direction of the sound. However, using the FFT enables determination of how the frequency content changes with time. The analysis of the Doppler shift of the frequency collected from one sensor permits an estimation of the velocity and range of the source.

Table 4
Statistics Concerning the Field Data

Item	Statistic
Location:	Vicksburg Municipal Airport
Date:	June 21, 1990
Time:	16:23 Central Daylight Time
Test No.	21
Audio phone:	Bruel & Kjaer, Model 4921
Channel:	1
Amplifier gain:	2
Digitizing rate:	2,048 samples/sec
Recording length:	135 sec
Source:	Helicopter with basic frequency 17.2 Hz
Altitude:	152.4 m
Horizontal offset at CPA:	100.0 m east
Source velocity:	33.5 m/sec
Travel direction and range:	2 km south to 2 km north of CPA
Temperature:	33.85 °C
Relative humidity:	56.58% (3 m above ground)
Barometric pressure:	1,071 millibars
Wind velocity:	0.641 m/sec
Sound velocity (calculated):	352.6 m/sec

Signal characteristics

The data were digitized at 2,048 samples per second, yielding a Nyquist frequency[1] of 1,024 Hz. Successive 1-sec-long sections of the data were analyzed using the FFT to compute the frequency content for that time interval. This permits a frequency resolution of 1 Hz.

A detailed plot of the amplitude as a function of time interval and frequency is illustrated in Figure 11. The time interval from the beginning of the test at time 1 until 135 sec later is plotted against the frequency content from 1 to 59 Hz. Each grid point on the 3-D surface represents the FFT amplitude (using a linear scale) for a 1-Hz increment of a 1-sec-long

---

[1] A frequency associated with the rate of digitization. Frequencies larger than the Nyquist frequency must be removed before digitization (Sheriff 1984).

interval. The higher the point, the larger the amplitude. The maximum value was 0.900.[1] All amplitudes below a threshold value of 0.033 were set to zero.

A number of bands of energy show the expected signature of Doppler-shifted acoustic energy from a source traveling in a straight line. From time 10 sec to 65 sec, the strongest frequency remains approximately constant at 19 Hz with the amplitude increasing. At this time the aircraft was approaching from the far field: for all practical purposes from the acoustic sensor's point of view, the aircraft was heading straight toward the sensor. The next section will present a more detailed calculation of this frequency.

From 65 sec to 80 sec, the frequency decreases steadily while the amplitude rises to its maximum and then starts to fall. In this period (at approximately 71 sec) the helicopter passes CPA. The slow drop in frequency guarantees that the aircraft will pass the sensor at some non-zero range. The slower the drop in frequency, the farther the range will be at CPA. The key piece of information necessary in this segment is the slope of the frequency curve.

From 80 sec to 120 sec, the frequency remained approximately constant again at between 15 and 16 Hz. The amplitude was decreasing also. At this time the aircraft was in the far-field retreating configuration: from the acoustic sensor's point of view, the aircraft was going directly away from the sensor. Since the frequency falls almost halfway between two integer frequency values, the accurate calculation of this frequency can result in problems concerning which frequency bin to select.

Approaching Fundamental Signal - 19.10 Hz

When one considers the approaching signal in the time interval, [30,45], from 30 to 45 sec into Run 21, the signal-to-noise ratio is high, and the frequency still appears to be constant. This is the appropriate time to determine the far-field approaching frequency.

Complex plane of the FFT

Table 5 shows the FFT amplitudes near the end and coherence over the entire time interval for a number of frequencies close to the dominant energy at 19 Hz. Although the two largest amplitudes are usually the 19 and

---

[1] The units of the amplitude are a scalar multiple of microbars. The scalar was applied to obtain the maximum dynamic range of signal from the analog to digital processing step.

Table 5
Far-Field Approaching FFT Amplitude of a Helicopter

Frequency (Hz)	Coherence [30,45]	Time Intervals (sec) of FFT Analysis					
		[38,39]	[39,40]	[40,41]	[41,42]	[42,43]	[43,44]
10.0	0.178	0.007	0.012	0.014	0.022	0.007	0.029
11.0	0.002	0.044	0.019	0.030	0.011	0.010	0.015
12.0	0.002	0.046	0.014	0.014	0.012	0.008	0.011
13.0	0.047	0.025	0.021	0.010	0.009	0.004	0.027
14.0	0.040	0.019	0.005	0.009	0.002	0.011	0.027
15.0	0.240	0.011	0.016	0.013	0.004	0.013	0.002
16.0	0.291	0.012	0.018	0.004	0.011	0.013	0.010
17.0	0.088	0.018	0.017	0.004	0.012	0.014	0.014
18.0	0.047	0.015	0.009	0.012	0.008	0.016	0.010
19.0	0.700	0.071	0.082	0.100	0.105	0.106	0.070
20.0	0.160	0.018	0.008	0.017	0.017	0.035	0.008
21.0	0.080	0.014	0.004	0.010	0.011	0.010	0.012
22.0	0.175	0.003	0.006	0.002	0.003	0.002	0.003
23.0	0.000	0.006	0.001	0.005	0.002	0.005	0.001
24.0	0.032	0.011	0.006	0.002	0.005	0.005	0.007
25.0	0.011	0.012	0.005	0.006	0.004	0.007	0.001
26.0	0.083	0.004	0.001	0.003	0.004	0.006	0.002
27.0	0.056	0.000	0.003	0.003	0.001	0.004	0.003
28.0	0.126	0.006	0.005	0.005	0.009	0.002	0.005
29.0	0.171	0.008	0.003	0.005	0.004	0.002	0.005
30.0	0.321	0.007	0.007	0.004	0.001	0.006	0.009

20 Hz, the coherence .700 of the 19-Hz energy is much higher than the 20 Hz coherence of .160. (It must be noted that the coherence was calculated over all fifteen 1-sec intervals from 30 to 45 sec. Hence, it appears to contain much more information than shown in Table 5.) The phase (Table 6) appears to be much more challenging to interpret (even for the strong 19-Hz energy). The plot of the FFT of the 19-Hz energy in the complex plane is shown in Figure 12 for the time period from 30 to 45 sec. This graph shows the rotation of the successive points around the origin in a manner reminiscent of a pure cosine wave (see Figure 7).

Table 6
Far-Field Approaching FFT Phase (degrees) of a Helicopter

Frequency (Hz)	Coherence [30,45]	Time Intervals (sec) of FFT Analysis					
		[38,39]	[39,40]	[40,41]	[41,42]	[42,43]	[43,44]
14.0	0.040	68.7	129.5	176.4	-53.6	-90.0	13.1
15.0	0.240	-113.4	-131.2	-168.2	111.4	-95.8	128.8
16.0	0.291	-143.9	-95.2	19.8	-9.3	-58.1	110.7
17.0	0.088	-145.8	62.8	-47.7	134.0	26.4	3.6
18.0	0.047	-79.2	146.4	-135.0	-114.3	-75.2	-175.3
19.0	0.700	-154.7	-139.4	-113.1	-89.2	-57.0	-20.9
20.0	0.160	-133.0	-176.8	117.5	104.9	113.7	39.1
21.0	0.080	-41.7	89.4	91.7	92.4	117.5	-1.5
22.0	0.175	-0.7	-11.9	5.0	85.1	90.6	-8.5
23.0	0.000	10.8	-79.9	53.5	-41.5	140.0	-94.7
24.0	0.032	37.9	-69.7	4.4	155.5	139.4	125.6
25.0	0.011	21.1	3.3	145.1	-55.5	147.7	39.3

Complex plane of the CSD

The CSD of successive time intervals is plotted in Figure 13. The CSD is obtained by multiplying the two FFT amplitudes and taking the difference between the two FFT phases of adjacent time intervals. The roughly constant rotation of the FFT phase is translated to the CSD as the points roughly all plotting at a constant angle (the rotation angle) to the positive real axis. All of the large amplitude points fall in the first quadrant (positive real and imaginary parts). This fact is exploited when a number of adjacent CSD values are added together.

Cumulative sum of the CSD

Figure 14 plots the cumulative sums of the CSD values of adjacent intervals: The first point, the CSD value that compares [0,1] to [1,2], is connected to the point that is the complex sum of the first two CSD values. The line that connects these two points actually represents the second CSD complex number. This process is continued until all 14 of the CSD values are added together. Table 7 summarizes the calculation of the cumulative sum of the CSD for the 19-Hz energy.

**Table 7
Calculation of the Cumulative Sum of the Cross-Spectral
Density for 19 Hz Far-Field Approaching Helicopter**

Time	Intervals		Cross-Spectral Density		Cumulative Sum	
	First	Second	Real	Imaginary	Real	Imaginary
31	[30,31]	[31,32]	0.000435	-0.000545	0.000435	-0.000545
32	[31,32]	[32,33]	-0.000395	0.001141	0.000040	0.000596
33	[32,33]	[33,34]	0.001673	0.003371	0.001713	0.003966
34	[33,34]	[34,35]	0.005093	0.000698	0.006806	0.004664
35	[34,35]	[35,36]	0.003188	0.005995	0.009994	0.010659
36	[35,36]	[36,37]	0.001883	-0.001213	0.011877	0.009446
37	[36,37]	[37,38]	0.000653	0.002739	0.012530	0.012185
38	[37,38]	[38,39]	0.003143	0.005400	0.015673	0.017585
39	[38,39]	[39,40]	0.005616	0.001536	0.021288	0.019121
40	[39,40]	[40,41]	0.007351	0.003633	0.028639	0.022755
41	[40,41]	[41,42]	0.009600	0.004254	0.038239	0.027009
42	[41,42]	[42,43]	0.009418	0.005931	0.047657	0.032940
43	[42,43]	[43,44]	0.005995	0.004372	0.053652	0.037311
44	[43,44]	[44,45]	0.002681	0.004837	0.056333	0.042148

Interpretation of approaching sound frequency

The final point $X=.056333 + .042148i$ of Figure 14 represents the vector sum of the real and imaginary components of the 14 individual CSD values. The direction of this point from the origin represents the CSD amplitude weighted sum of angles of the individual CSD vectors and is, therefore, the best representation of the change of the approaching signal from a pure 19-Hz component. Using Equation 20, the approaching far-field frequency f_a can be calculated more accurately as

$$f_a = 19.00 \ Hz + \frac{arctan \left(\dfrac{0.042148}{0.056333} \right) cycles}{1 \ sec}$$

$$= 19.00 \ Hz + \frac{(36.80 \ deg) \cdot \dfrac{1 \ cycle}{360 \ deg}}{1 \ sec} \tag{23}$$

$$= 19.10 \ Hz$$

The value $f_a = 19.10$ Hz can be considered as the average frequency of the approaching coherent energy falling near 19 Hz over the time period [30,45]. The degree of accuracy is presently undetermined, but the good alignment of the individual vectors that form the cumulative sum (Figure 14) suggests that the above number is accurate to within 0.1 Hz. (The additional precision implied in 19.10 Hz will be retained because of the sensitive nature of some future calculations.)

Another test of accuracy uses Equation 20 on each of the 14 CSD measurements to determine how much the actual frequency implied by the phase of the individual CSD values varies over that length of time. Figure 15 summarizes the results. Most of the individual frequencies fall between 19.0 and 19.2 Hz. The first two CSD values (when 20 Hz had a larger amplitude) increased the mean to 19.15 Hz and the standard deviation to .16 Hz. (Ignoring those first two CSD values, the mean and standard deviation become 19.10 and .08 Hz, respectively. This would agree with Equation 23, which is a 19-Hz-amplitude weighted sum of CSD complex numbers.)

Comparison with neighboring frequencies

Amplitudes. The main energy of the CSD and FFT is concentrated at 19 Hz in the time period [33,45] (Table 5). The fact that the 19-Hz FFT amplitude is over three times larger than the amplitudes of 15 to 18 and 20 to 30 Hz in [38,44] suggests that analyzing the 19-Hz FFT and CSD information is sufficient to determine the approaching frequency of the source (Figure 16).

Coherences. The coherence (Table 5 and Figure 17) of the 1-sec-long intervals composing the total interval [30,45] is another good indicator that the 19-Hz frequency is the only FFT and CSD energy that should be considered. Of all the frequencies between 10 and 30 Hz, only the 19-Hz component had a coherence above 0.325 over the entire 15-sec-long time period [30,45]. At 0.700, the 19-Hz coherence was more than twice as large as the maximum of those other frequencies. (Because the 18-Hz coherence is 0.047 and the 20 Hz is 0.160, far below the 19-Hz level, these frequencies must not be used in the far-field analysis. This result for the approaching signal was significantly different from the situation for the retreating signal, where frequencies adjacent to the maximum amplitude frequency also needed to be analyzed.)

Retreating Fundamental Signal - 15.65 Hz

The retreating far-field signal vastly differed from the approaching far-field signal. As Figure 11 indicates, the approaching signal was evident at about 60 sec before the CPA. However, the retreating signal has dropped off the threshold of the graph within 30 sec after the CPA. For this reason,

the analysis of the retreating signal was performed much closer to the CPA in the interval [90,105].

Comparison of neighboring frequencies

Amplitudes. The strong energy in this time interval was around 15 and 16 Hz. The maximum energy was at 16 Hz, with 15 Hz in second place at about 50 percent of maximum; third was 17 Hz at roughly 30 percent of maximum. Table 8 summarizes the amplitude for a selected portion of this time period. The corresponding phase information is given in Table 9.

Table 8
Far-Field Retreating FFT Amplitude of a Moving Helicopter

Frequency (Hz)	Coherence [90,105]	Time Intervals (sec) of FFT Analysis					
		[90,91]	[91,92]	[92,93]	[93,94]	[95,96]	[97,98]
10.0	0.150	0.013	0.015	0.013	0.008	0.004	0.006
11.0	0.051	0.004	0.007	0.019	0.009	0.005	0.013
12.0	0.088	0.010	0.010	0.008	0.011	0.003	0.012
13.0	0.632	0.011	0.013	0.016	0.010	0.011	0.009
14.0	0.607	0.017	0.014	0.027	0.019	0.020	0.021
15.0	0.717	0.056	0.054	0.040	0.051	0.041	0.055
16.0	0.877	0.109	0.101	0.109	0.087	0.081	0.082
17.0	0.712	0.034	0.034	0.023	0.020	0.025	0.028
18.0	0.376	0.021	0.008	0.011	0.012	0.014	0.027
19.0	0.371	0.047	0.027	0.026	0.007	0.032	0.027
20.0	0.170	0.041	0.029	0.018	0.028	0.033	0.010
21.0	0.429	0.013	0.015	0.011	0.005	0.010	0.003
22.0	0.402	0.009	0.013	0.004	0.011	0.005	0.004
23.0	0.150	0.006	0.007	0.005	0.011	0.005	0.007
24.0	0.179	0.004	0.010	0.006	0.005	0.001	0.006
25.0	0.002	0.002	0.012	0.008	0.006	0.001	0.007

Table 9
Retreating FFT Phase (degrees)[1] of a Moving Helicopter

Frequency (Hz)	Coherence [90,105]	Time Intervals (sec) of FFT Analysis					
		[90,91]	[91,92]	[92,93]	[93,94]	[95,96]	[97,98]
10.0	0.179	-118.4	102.8	30.2	-36.0	157.7	-21.7
11.0	0.094	-98.9	152.3	-1.4	-15.2	-173.1	86.5
12.0	0.141	-123.2	164.9	4.1	-17.3	131.9	45.4
13.0	0.710	-120.6	119.7	40.6	-69.8	147.5	51.9
14.0	0.709	-101.6	153.7	10.7	-71.1	149.3	48.1
15.0	0.768	-114.9	144.5	3.2	-82.1	176.9	40.9
16.0	0.893	71.1	-50.0	-152.9	92.2	-11.6	-144.2
17.0	0.781	72.0	-52.9	-137.1	132.6	-13.7	-109.3
18.0	0.593	48.2	-40.1	-154.9	72.0	0.1	-129.4
19.0	0.580	47.0	-161.3	-85.1	-26.0	80.6	-112.7
20.0	0.261	165.4	20.7	155.9	53.5	-64.3	58.1
21.0	0.581	130.7	-6.4	-178.6	76.8	-27.8	165.1
22.0	0.644	153.3	-23.2	-175.1	68.9	-39.6	130.2
23.0	0.186	-143.0	12.8	-179.8	87.9	-64.1	171.7
24.0	0.254	82.4	-33.7	-178.9	122.7	88.3	-177.9
25.0	0.003	-79.6	-48.1	-169.3	-24.8	-11.5	-170.2

[1] A table of factors for converting non-SI units of measurement to SI units is presented on page vi.

Coherences. Unlike the approaching signal, the coherence remained above 0.70 for all three of the FFT frequencies of 15, 16, and 17.

Cumulative sums of the CSD. Because of the adequate amplitude and good coherence, all three of these frequencies were analyzed using the cumulative sums of CSD (Figure 18). If the different amplitudes are ignored, all three frequencies show approximately the same shaped curve.

Frequency calculations

Table 10 lists the actual cumulative sum of CSD of individual FFT frequencies, coherence, and the implied frequency change calculated from Equation 20.

Table 10 Calculation of Retreating Far-Field Frequency					
Frequency hertz	Coherence	Cumulative Sum CSD		Implied Angle Change	
		Real	Imaginary	degrees	cycles
15	0.717	-0.011426	-0.013759	-129.71	-0.360
16	0.877	-0.032258	-0.049309	-123.19	-0.342
17	0.712	-0.003260	-0.005241	-121.88	-0.339
Vector Sum		-0.046944	-0.068309	-124.50	-0.346

Interpretation

Since all of the three significant frequencies look similar, the vector sum (Figure 19) probably represents the best approximation of the total signal. Note that this sum applies weights appropriate to the respective amplitudes of each of the individual signals. Since 16 Hz has the largest amplitude, most likely the final change number represents the shift from 16 Hz.

$$f_r = retreating frequency = 16 - 0.35 = 15.65 Hz \qquad (24)$$

Because the absolute value of the angle change is close to 0.5 cycle, it is best to check the frequency of the second-largest amplitude (to guarantee that the answer is not 16.65 Hz). Since the 15-Hz amplitudes are second largest behind the 16 Hz, the energy can be expected to fall between 15 and 16 Hz as the calculated f_r satisfies.

4 Combination of Both Frequencies for the Fundamental

Basic Frequency Calculation

The combined knowledge of both the approaching and retreating frequencies permits the calculation of both the basic frequency of the helicopter and its velocity (under the assumptions of Table 1). The values of f_a and f_r (Equations 23 ? . ' +) can be inserted into Equation 3 to yield an estimate of the basic frequency f_0 that the helicopter would generate if it were not moving:

$$f_o = \frac{2 f_a f_r}{f_a + f_r} = \frac{2 \cdot 19.10 \cdot 15.65}{19.10 + 15.65}$$

(25)

$$= 17.21 \; Hz$$

This corresponds to the reported value of 17.2 Hz, four times the frequency of rotation of the main rotor shaft. With four blades on that rotor, the dominant energy in Figure 11 appears to be caused by the main rotor blades. The passive acoustic sensor analysis has correctly detected this frequency.

Since the microphone is measuring this frequency when the helicopter is at CPA, Figure 5 indicates that CPA occurred sometime around 70 sec into Run 21.

Velocity Estimation

Likewise, the velocity of the source can be estimated using Equation 4 or 6.

$$V = C \cdot \frac{f_a - f_o}{f_a}$$

$$= 352.6 \ ^m/_{sec} \cdot \frac{19.10 - 17.21}{19.10} \tag{26}$$

$$= 35.0 \ ^m/_{sec}$$

The formula requires only the knowledge of the approaching frequency f_a, the basic frequency f_o, and the velocity of sound C. This formula implies that if the basic frequency f_o were known while the helicopter was still in the far-field-approaching situation, the velocity could be calculated as soon as the approaching far-field frequency f_a could be determined. In Run 21 this frequency was calculated using the data from 30 to 45 sec (see "Approaching Fundamental Signal - 19.10 Hz," pp 21-25) long before the helicopter reached CPA at after 70 sec. Hence the velocity of the incoming helicopter could be estimated over 25 sec before it reached CPA. The actual number compares favorably with the velocity of 65 knots (33.5 m/sec) reported by the pilots. These results apply to this data set. The accuracy of the approaching velocity estimate, the time before CPA that it can be calculated, and the length of the time intervals required in the calculation are all dependent on the amount of background noise, the amplitude of the incoming signal, the quality of acoustic recording equipment, and the possible presence of other targets. The investigation of the limitations of the velocity formula is a fertile area for study —but remains outside the scope of this report.

30

5 Analysis of the CPA Frequencies for the Fundamental

Calculation of the Frequency at One Time

With the estimates of basic frequency $f_0 = 17.21$ Hz from Equation 25 and the velocity of the helicopter $V = 35.0$ m/sec (Equation 26), the time of CPA and range at CPA can be estimated from the CSD data of Table 11. The aircraft was at CPA when it generated a frequency f_0 at the receiver.

The FFT Amplitude part of Table 11 suggests that the signal crosses through 17.21 Hz during the interval [71,72]. Therefore, the detailed analysis of the frequency using Equation 20 on the 17-Hz component of the CSD that compares the [70,71] to [71,72] should generate the range estimate. The results will be considered applicable to 71 sec. For 17 Hz:

CSD Ampl 71 = (FFT Ampl [70,71]) (FFT Ampl [71,72])

$$= (0.407) \ (0.873) = 0.355311$$

CSD Phase 71 = (FFT Phase [71,72]) - (FFT Phase [70,71])

$$= (-104.9) - 171.3 \ deg = -276.2 \ deg$$

$$= 360.0 - 276.2 \ deg = 83.8 \ deg$$

$$= 83.8 \ deg \ (1 \ cycle/360 \ deg)$$

$$= 0.23 \ cycle$$

Since the 17-Hz CSD amplitude is an obvious maximum for all of the CSD frequencies from 15 Hz to 20 Hz of the time 71 sec, Equation 20 suggests that the dominant frequency $f(71)$ of the signal at 71 sec is

Table 11
Calculation of Frequency Near CPA

Frequency	Coherence [60,75]	FFT Amplitude					
		[67,68]	[68,69]	[69,70]	[70,71]	[71,72]	[72,73]
15.0	0.425	0.049	0.017	0.010	0.084	0.048	0.185
16.0	0.488	0.090	0.017	0.009	0.155	0.082	0.460
17.0	0.018	0.134	0.046	0.074	0.407	0.873	0.877
18.0	0.075	0.393	0.415	0.370	0.339	0.108	0.216
19.0	0.339	0.375	0.050	0.016	0.158	0.032	0.095
20.0	0.197	0.129	0.021	0.064	0.067	0.085	0.144

Frequency	Coherence [60,75]	FFT Phase, degrees					
15.0	0.425	2.4	131.3	-61.1	150.1	159.4	24.4
16.0	0.488	19.6	-64.7	-157.1	144.4	-165.5	34.6
17.0	0.018	32.6	128.8	-39.6	171.3	-104.9	-151.4
18.0	0.075	33.5	143.6	118.1	-30.5	129.1	-153.7
19.0	0.339	-147.8	-2.9	155.7	-23.9	88.1	-158.4
20.0	0.197	-122.4	100.1	43.6	-61.7	-11.4	-172.3

Frequency	Coherence [60,75]	CSD Amplitude				
		68	69	70	71	72
15.0	0.425	0.00083	0.00017	0.00084	0.00403	0.00888
16.0	0.488	0.00153	0.00015	0.00140	0.01271	0.03772
17.0	0.018	0.00616	0.00340	0.03012	0.35531	0.76562
18.0	0.075	0.16310	0.15355	0.12543	0.03661	0.02333
19.0	0.339	0.01875	0.00080	0.00253	0.00506	0.00304
20.0	0.197	0.00271	0.00134	0.00429	0.00570	0.01224

Frequency	Coherence [60,75]	CSD Phase, degrees				
15.0	0.425	128.9	-192.4	211.2	9.3	-135.0
16.0	0.488	-84.3	-92.4	301.5	-309.9	200.1
17.0	0.018	96.2	-168.4	210.9	-276.2	-46.5
18.0	0.075	110.1	-25.5	-148.6	159.6	-282.8
19.0	0.339	144.9	158.6	-179.6	112.0	-248.5
20.0	0.197	222.5	-56.5	-105.3	50.3	-160.9

Frequency	Coherence [60,75]	CSD Phase, cycles				
15.0	0.425	0.358	0.466	-0.413	0.026	-0.375
16.0	0.488	-0.234	-0.257	-0.163	0.139	-0.444
17.0	0.018	0.267	-0.468	-0.414	0.233	-0.129
18.0	0.075	0.306	-0.071	-0.413	0.443	0.214
19.0	0.339	0.403	0.441	-0.499	0.311	0.315
20.0	0.197	-0.382	-0.157	-0.293	0.140	-0.447
Interpretation, Hz		18.306	17.929	17.587	17.233	16.871

$$f(71) = 17\ Hz + \frac{0.23\ cycle}{1\ sec} = 17.23\ Hz$$

The value, calculated from the CSD values of [70,71]:[71,72], can be checked against the origina¹ FFT results for [70,71] and [71,72]. The amplitude of the FFT of [70,71] is .407 at 17 Hz and .339 at 18 Hz (Table 11), suggesting that the main frequency at time 70.5 is roughly halfway between 17 and 18 Hz — but closer to 17 Hz. So the FFT of [70,71] suggests that f(70.5) ≈ 17.4 Hz. Similarly, the FFT of [71,72] suggests that f(71.5) ≈ 17 1 Hz, since the amplitude of 18 Hz is slightly larger than that of 16 Hz. Taking the average of these two approximations of the frequencies of the FFT's yields an average of 17.25 Hz for an f(70). Hence the individual FFT amplitudes of the 1-sec-long intervals compare well with the CSD calculation of 17.23 Hz for the boundary between the time intervals.

Frequency Estimate as a Function of Time

The interpretation of the frequency of the dominant energy was made for all of the times from 61 to 74 sec (see Figure 20). The calculation of the frequencies from 68 to 72 sec is shown in Table 11. These calculations were made using the FFT frequency at the largest amplitude. The smooth graph in Figure 20 suggests that the frequency calculation is robusι (i.e., not subject to large errors resulting from noise in the data).

The time t_0 when the sound reaches the receiver of the helicopter at CPA can be estimated using Equation 10 and the straight lines through successive points t-1 and t for the time increment of 1 sec of Figure 20. This calculation is based on the intersection of the basic frequency f_0 with the linear interpolation of the Doppler-shifted frequency as a function of time.

$$t_o(t) = t + \frac{f_o - f(t)}{\frac{df}{dt}(t)}$$

$$t_o(t) = t + \left[\frac{17.21\ Hz - f(t)}{f(t) - f(t - 1)}\right] \cdot (1\ sec)$$

This formula is evaluated in Table 12 using the interpreted frequencies from the bottom of Table 11. All of the values are close. The time of CPA of 71.07 sec will be used for the estimate for the main rotor blades. Since this time was reasonably estimated before the helicopter reached CPA, the time of CPA can be calculated sufficiently early to decide on a response to this incoming target.

**Table 12
Estimates of the Time of CPA**

Time t of Second Point of Slope, sec	Slope, Hz/sec	Estimate of CPA t_o(t), sec
69	-0.38	70.92
70	-0.34	71.11
71	-0.35	71.07
72	-0.36	71.07

Calculation of the Range Using the Slope

The slope of the frequency as a function of time (Figure 20) appears to remain roughly constant from 68 sec to 74 sec. This means that the formula for the range at CPA, which requires the slope at CPA, can be evaluated using the approximations of the slope before the helicopter reaches CPA. The main rotor prediction line of Figure 21 is the application of Equation 5

$$R = \frac{-f_o \cdot V^2}{C \cdot \frac{df}{dt}(CPA)}$$

with current estimates of the data

$$R(t) = \frac{-17.21\ Hz \cdot (35.0\ ^m/_{sec})^2}{352.6\ ^m/_{sec} \cdot [f(t) - f(t-1)]\ /\ (1\ sec)} \tag{27}$$

The values near CPA, summarized in Table 13, are stable in the vicinity of 167 m even before the helicopter arrives at CPA. The estimated range given by the pilots was 182.3 m [100 m east (estimated) and 152.4 m vertical].

Summary of the Analysis of the Main Rotor Signal

The CSD analysis of the strong main rotor energy that initially fell around 19 Hz yielded a great deal of relevant information about the helicopter. The cumulative sum of the cross-spectral densities over the time intervals [30,45] and [90,105] yielded estimates of the approaching and retreating frequencies at 19.10 and 15.65 Hz, respectively. These values yielded the estimate of the basic frequency of 17.21 Hz, which agrees

Table 13
Estimates of the Range at CPA

Time t of Second Point of Slope, sec	Estimate of CPA Time, sec	Estimate of Range, m	Error of Range
69	70.92	158.4	-12.9%
70	71.11	174.6	-4.1%
71	71.07	168.7	-7.5%
72	71.07	165.0	-9.4%

with the known 17.2-Hz frequency of the four rotor blades of the helicopter. The basic frequency and the approaching frequency were combined to calculate the velocity of the aircraft as 35.0 m/sec, slightly above the reported 33.5 m/sec reported by the pilots (but less than some preliminary global positioning system (GPS) data).

Using the basic frequency and the slope of the Doppler-shifted frequency as a function of time curve, the time of CPA is estimated to be at approximately 71 sec into the run (Figure 20). The basic frequency, slope near CPA, and velocity estimates combine to predict the range 167 m at CPA (Figure 21). The rough estimate of the pilots was 182 m.

The CSD analysis estimated within acceptable tolerances the basic frequency (of the fundamental), velocity, time of CPA, and range of CPA of the moving helicopter. It is very significant that all of this information was derived solely from passive acoustic measurements at one microphone.

6 Conclusions and Recommendations

Conclusions

Passive acoustic energy can be used to estimate the velocity, range at CPA, and time of CPA from knowledge of the Doppler shift of frequency over time recorded at one acoustic receiver (Equations 5, 6, and 11). Formulas for these estimates require a high resolution of the frequency of the signal over relatively short time periods.

The traditional FFT frequency analysis is not sufficient in this dynamic situation; the CSD is shown to be much better than conventional FFT approaches. The phase, measured in cycles and divided by the length of the FFT interval, can be interpreted as the amount of the shift between the actual dominant energy and the frequency of the FFT calculation (Equation 20). For the dominant signal of the data, the CSD frequency resolution appeared to be within 0.1 Hz.

When the basic frequency (i.e., frequency before any Doppler shift) is known, the high resolution of the far-field approaching frequency of the dominant main rotor energy at 19 Hz permits a prediction of 35.0 m/sec for the approach velocity, accurate to within 5 percent of the value of 33.5 m/sec reported by the pilots. The analysis of this energy near CPA yielded range estimates of 158 to 175 m, accurate to within 13 percent of the range of 182 m reported by the pilots. Some of the sensor estimates were made before the helicopter reached CPA.

If nothing were known about the approaching aircraft, the basic frequency and all of the above information could be calculated to the same levels of accuracy by analyzing the far-field retreating frequency after the aircraft had moved far away. The combined knowledge of the far-field approaching frequency and the far-field retreating frequency yields an estimated basic frequency of 17.21 Hz. The specification of the helicopter is 17.2 Hz. The presence of two sensors, with one far out in front of the other, can provide resolution of the unknown frequency problem. If the sensor out front has the task of determining the basic frequency, then this

frequency can be passed to the second sensor to determine the range when the aircraft approached CPA.

Calculations provided herein used the data from one passive sensor on actual acoustic data. The first harmonic and the tail rotor energy provided additional measurements that represent independent statistical support of the main rotor calculations of velocity and range. Additional sensors add independent data. All of these measurements can greatly enhance the capability of using acoustic data to perform as a passive detection and ranging device.

Recommendations

The following is a list of topics recommended for future study:

a. Creation of a computer system to

    (1) detect and track coherent energy.

    (2) perform the above analysis automatically.

    (3) perform calculations on an 80386 PC in real time.

b. Integration of the computer system with

    (1) direction-finding programs.

    (2) wide-area mine (WAM) technology.

c. Further study of

    (1) FFT intervals of 0.5 sec and 0.25 sec.

    (2) faster moving sources.

        (a) close to the speed of sound.

        (b) faster than the speed of sound.

    (3) lower flying targets.

    (4) changing velocities of the aircraft.

    (5) impact of curvilinear flight paths.

    (6) effect of wind.

    (7) effect of multiple sources.

(8) impact of battlefield noise interference.

d. Identification of acoustic sources that emit a temporally coherent signal.

e. Creation of a list of the basic frequencies of each aircraft.

Such studies could lead to broad applications in both civil and military aircraft identification and tracking, and enhance current procedures.

References

Ahlfors, Lars V. 1966. *Complex Analysis*. New York: McGraw-Hill.

Cress, Daniel H., and Olson, Robert E. 1990. *Temporal Coherence and Temporal Phase Analysis: Emphasis on Helicopter Signatures*. 21st Meeting of NATO AC/243, Panel 3, RSG.11, Kjeller, Norway, 28 May - 1 June 1990.

Dudgeon, Dan E., and Mersereau, Russell M. 1984. *Multidimensional Digital Signal Processing*. Englewood Cliffs, NJ: Prentice-Hall.

Olson, Reo, and Cress, Daniel H. 1990. *Passive Range Estimation of a Moving Source*. 22nd Meeting of NATO AC/243, Panel 3, RSG.11, Vicksburg, Mississippi, October 29 - November 2, 1990.

Sheriff, Robert E. 1984. *Encyclopedic Dictionary of Exploration Geophysics*. 2nd ed. Tulsa, OK: Society of Exploration Geophysicists.

Smith, George. 1984. *Beam Forming Methods in Seismic Signal Arrays*. 16th Southeastern Symposium on System Theory, Starkville, Mississippi, March 25-27, 1984.

Stabler, J. R., Baylot, E. A., and Cress, D. H. 1976. Frequency Dependent Wave Arrival Time Delays in Dispersive and Nondispersive Media. In *Transactions of the twenty-first conference of army mathematicians*, ARO Report 76-1, pp 431-443.

Weidner, Richard T., and Sells, Robert L. 1965. *Elementary Classical Physics* 2: 1049-1056. Boston: Allyn-Bacon.
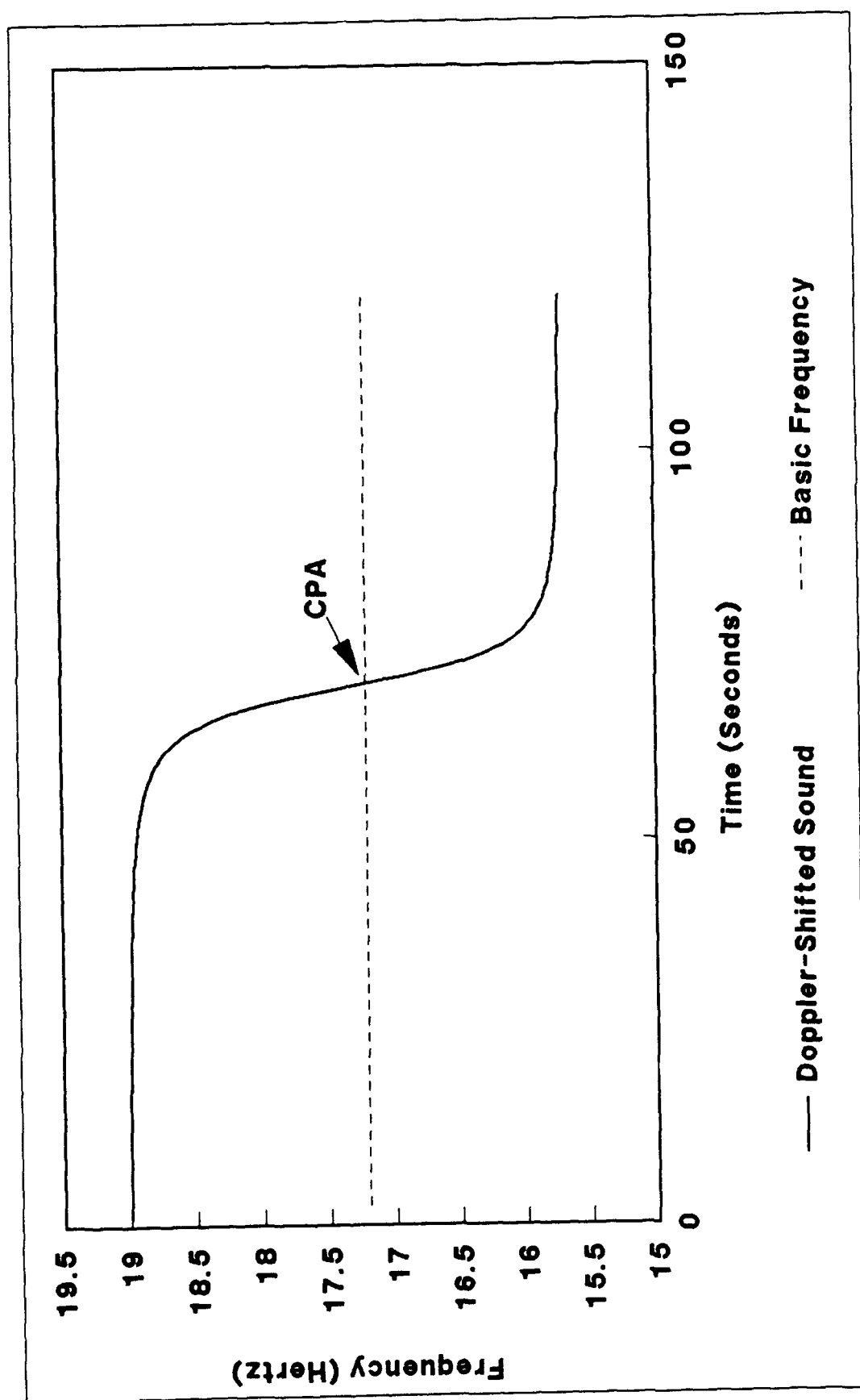
Figure 1. Simulation of the Doppler shift of a 17.2-Hz basic frequency caused by a sound source moving at 33.5 m/sec
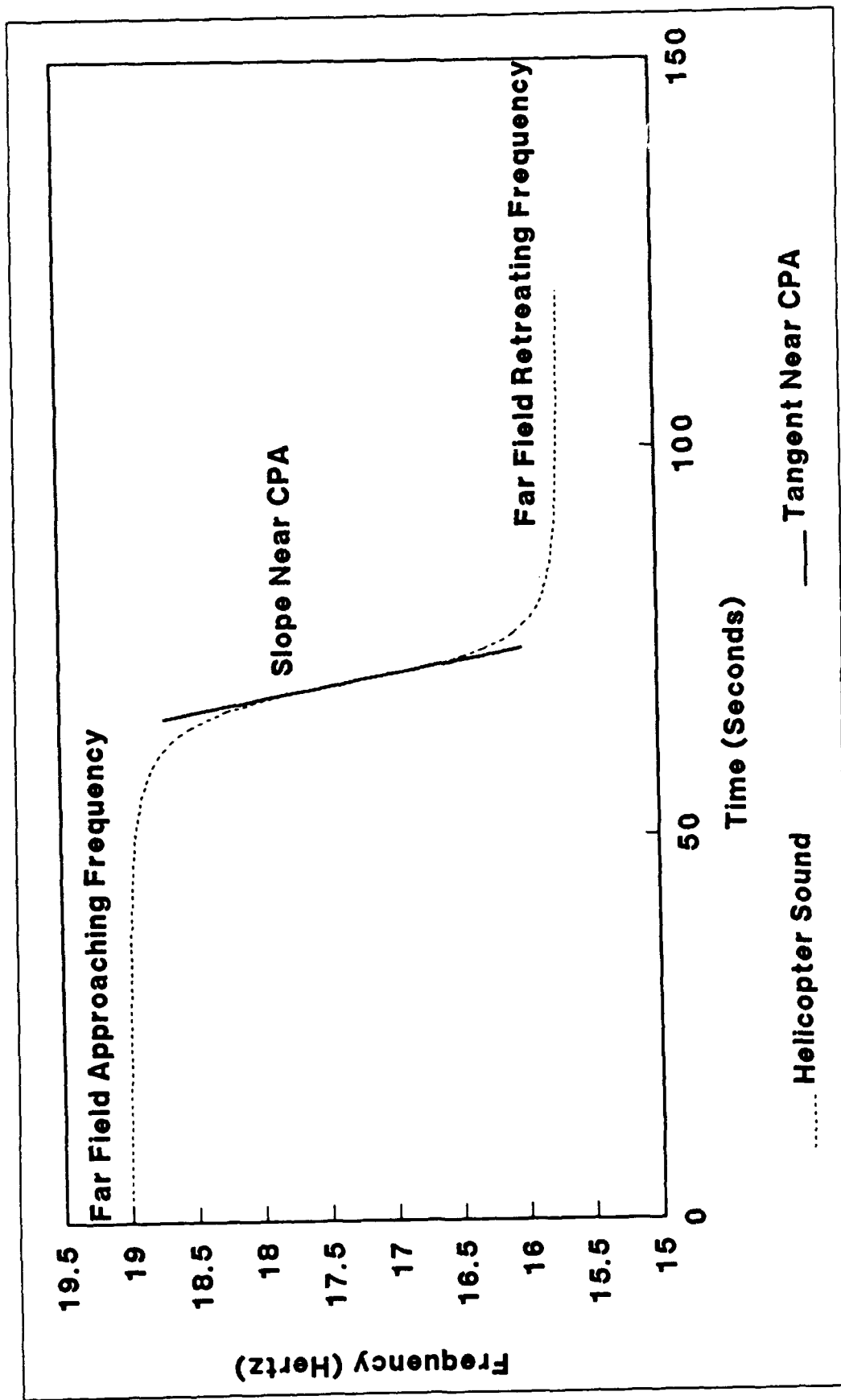
Figure 2. The key input data for passive estimation of velocity, range, basic frequency, and time of CPA if nothing is known about the helicopter

Velocity = 33.5 m/sec

Altitude = 152 m

Horizontal offset = 100 m

Basic frequency = 17.2 Hz

Time (Seconds)

Frequency (Hertz)

———— Transmitted from Helicopter   ·········· Received at Microphone
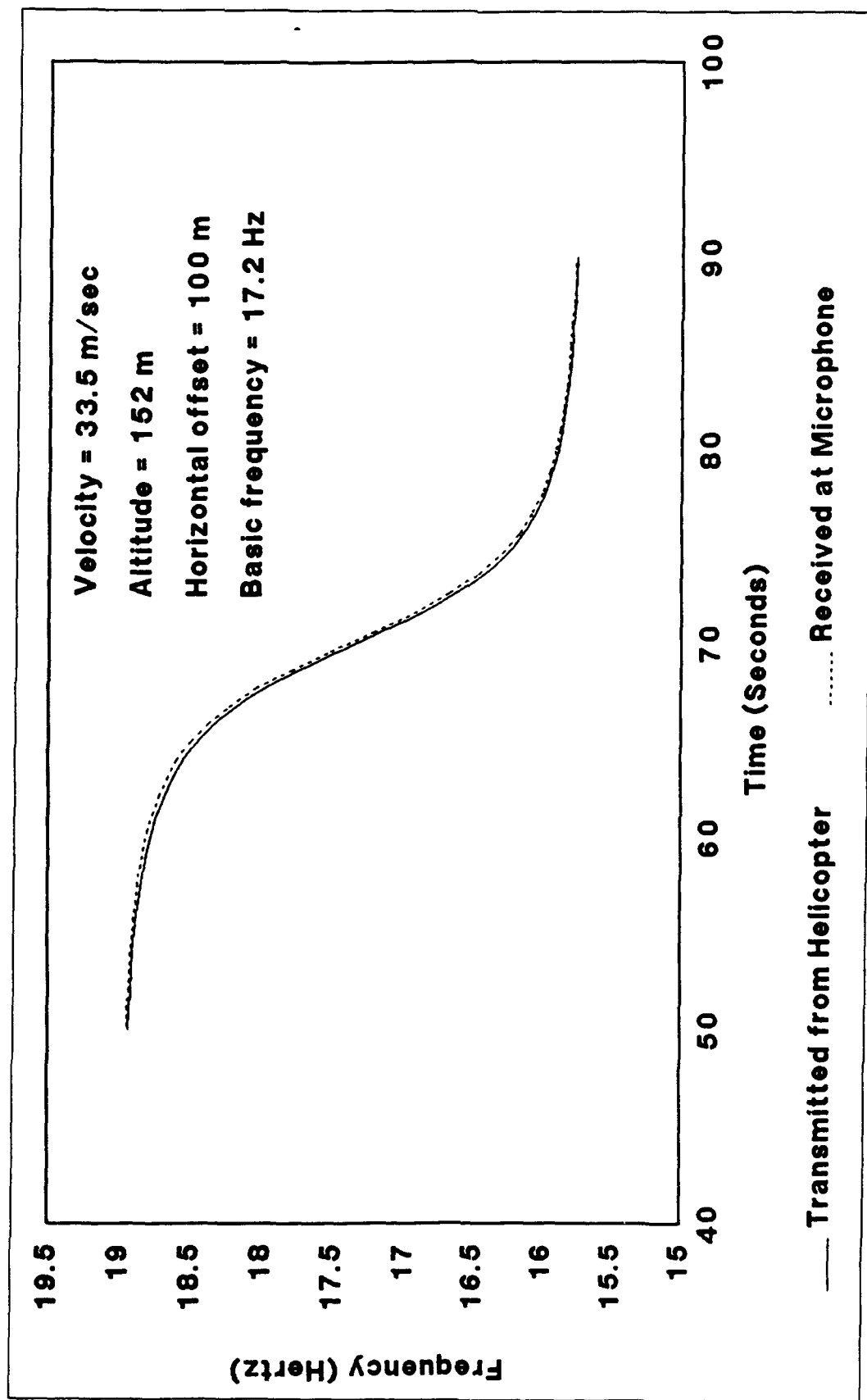
Figure 3. Viewpoint comparisons: source versus receiver from simulation of Doppler shift - Run 21
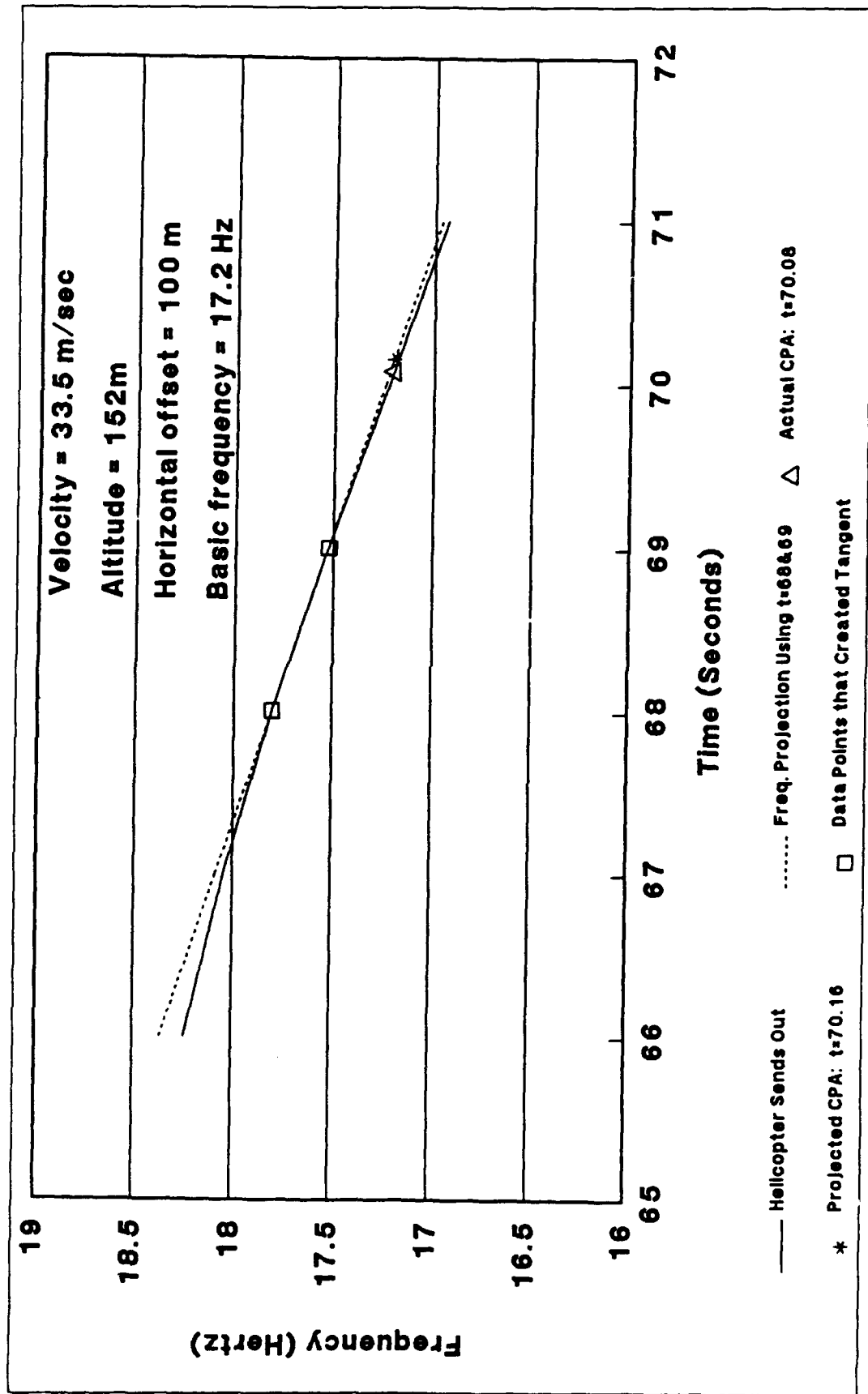
Figure 4. Calculation of time of CPA from simulation of Doppler shift - Run 21
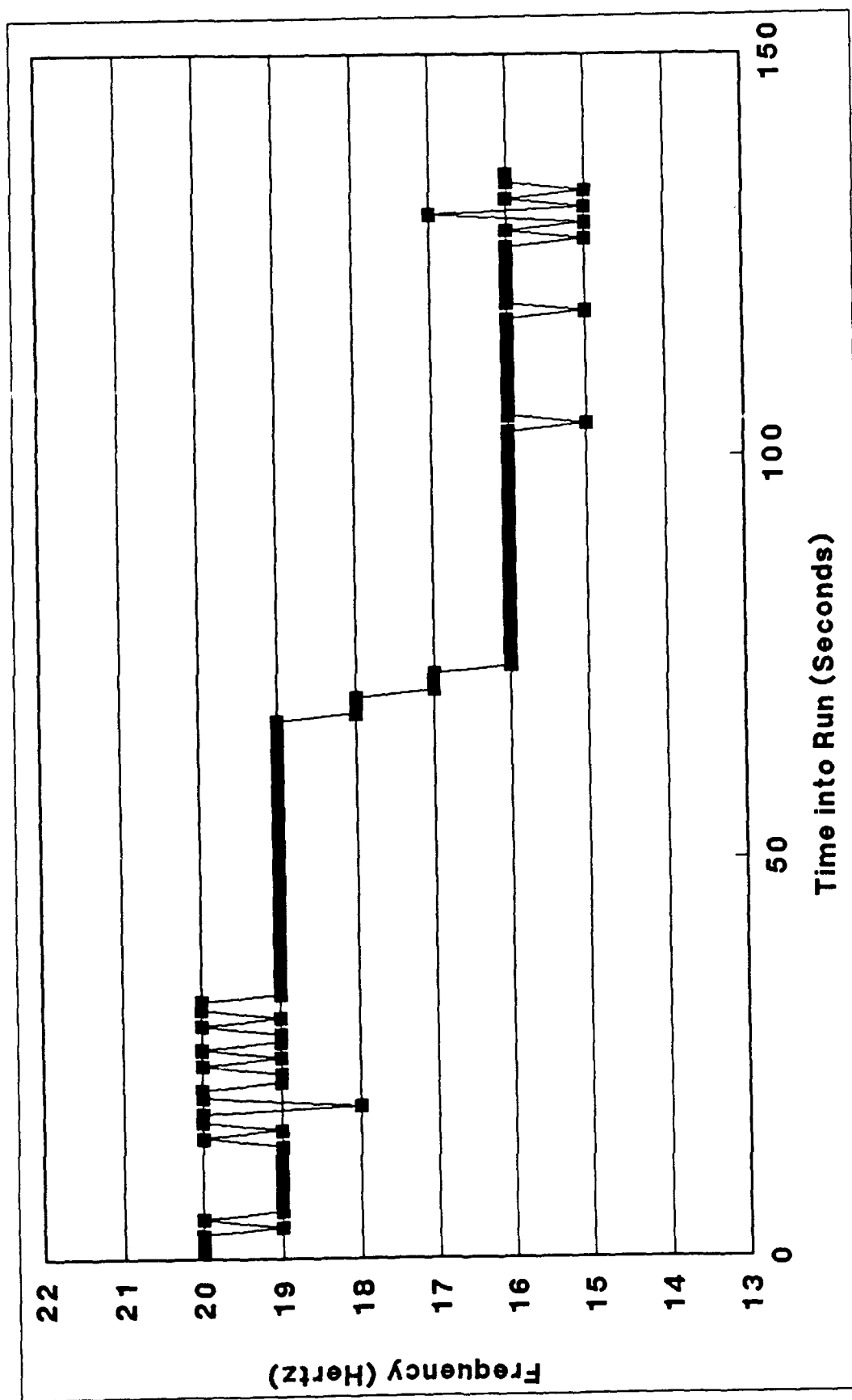
Figure 5. Frequency of maximum FFT amplitude (main rotor blades) of helicopter - Run 21
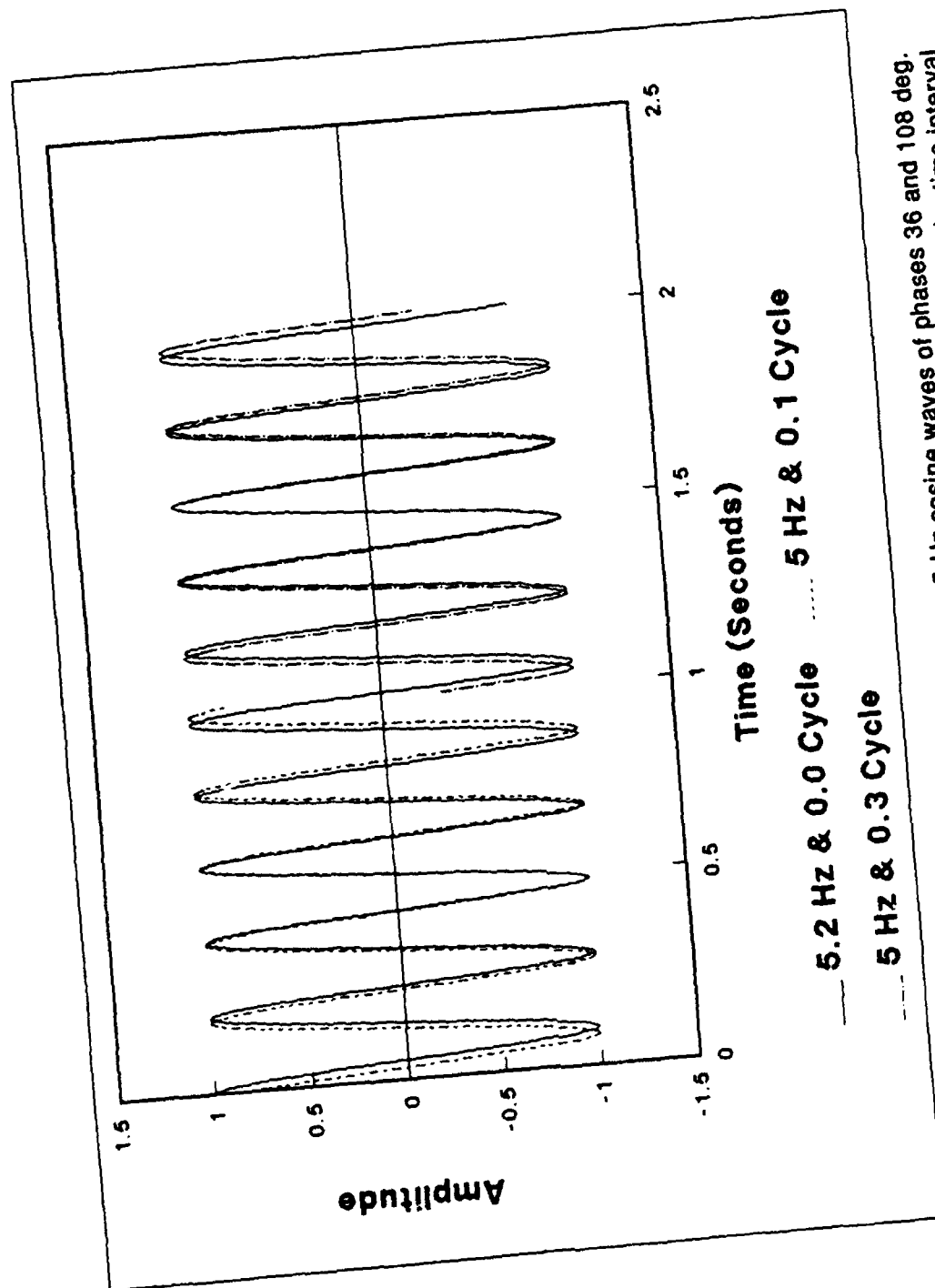
Figure 6. Curve fitting of a 5.2-Hz cosine wave by two 5-Hz cosine waves of phases 36 and 108 deg. The 5-Hz and 0.1-cycle curve is the best FFT fit of the 5.2-Hz and 0.0-cycle signal in the time interval [0,1]. Also, the 5-Hz and 0.3-cycle curve is the best FFT fit of the 5.2-Hz and 0.0-cycle signal in the time interval [1,2]. The difference, 0.2 cycle, between the two phases of the two 5-Hz FFT curves is caused by the fact that the frequency of the signal being fitted is 0.2-Hz different from those 5-Hz FFT curves
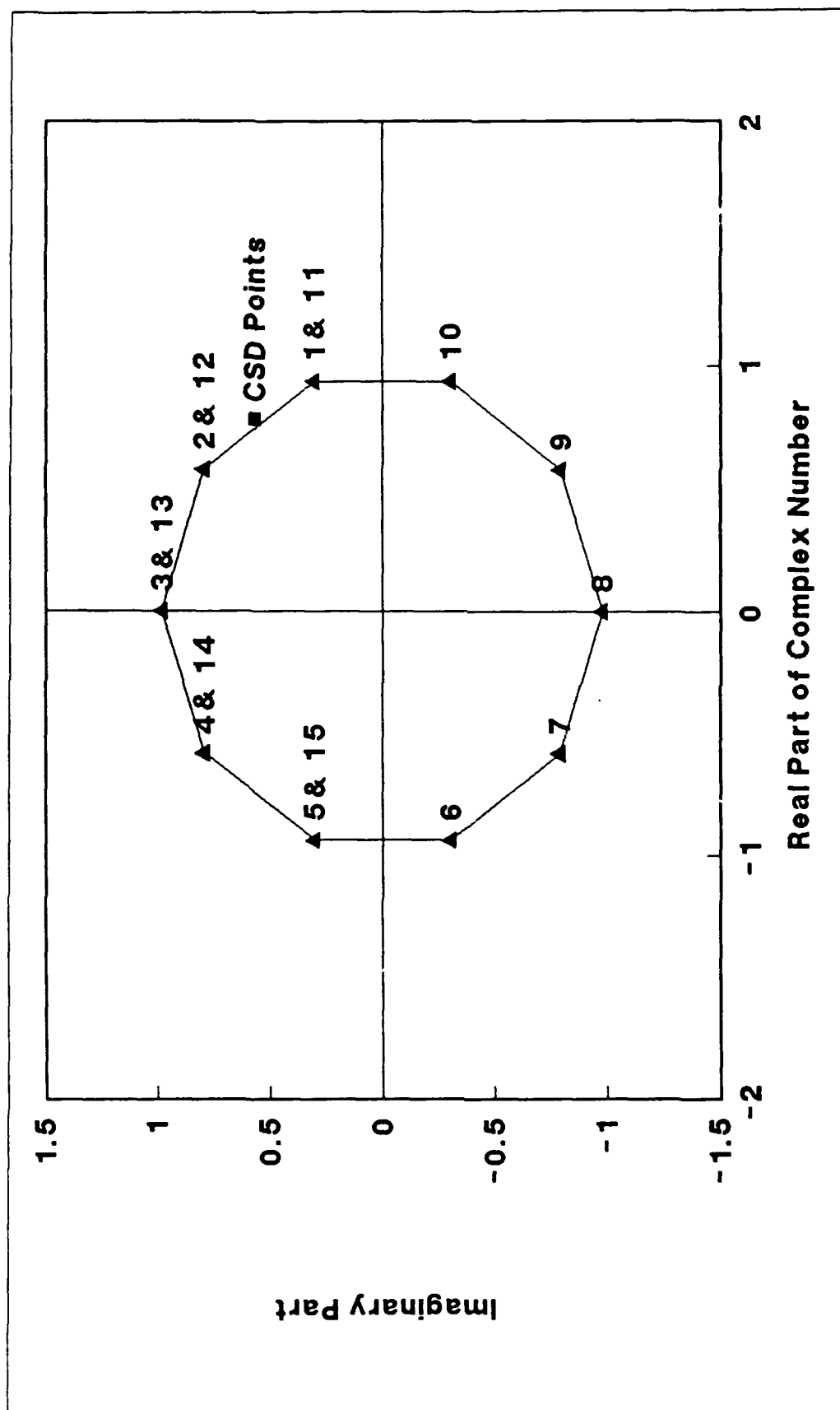
Figure 7. The 19-Hz FFT analysis of temporal coherence (input is a 19.1-Hz cosine wave). Note: coherence is 1.000. The label for each point represents the end of the 1-sec-long interval (e.g., 7 represents the FFT of the time interval [6,7])
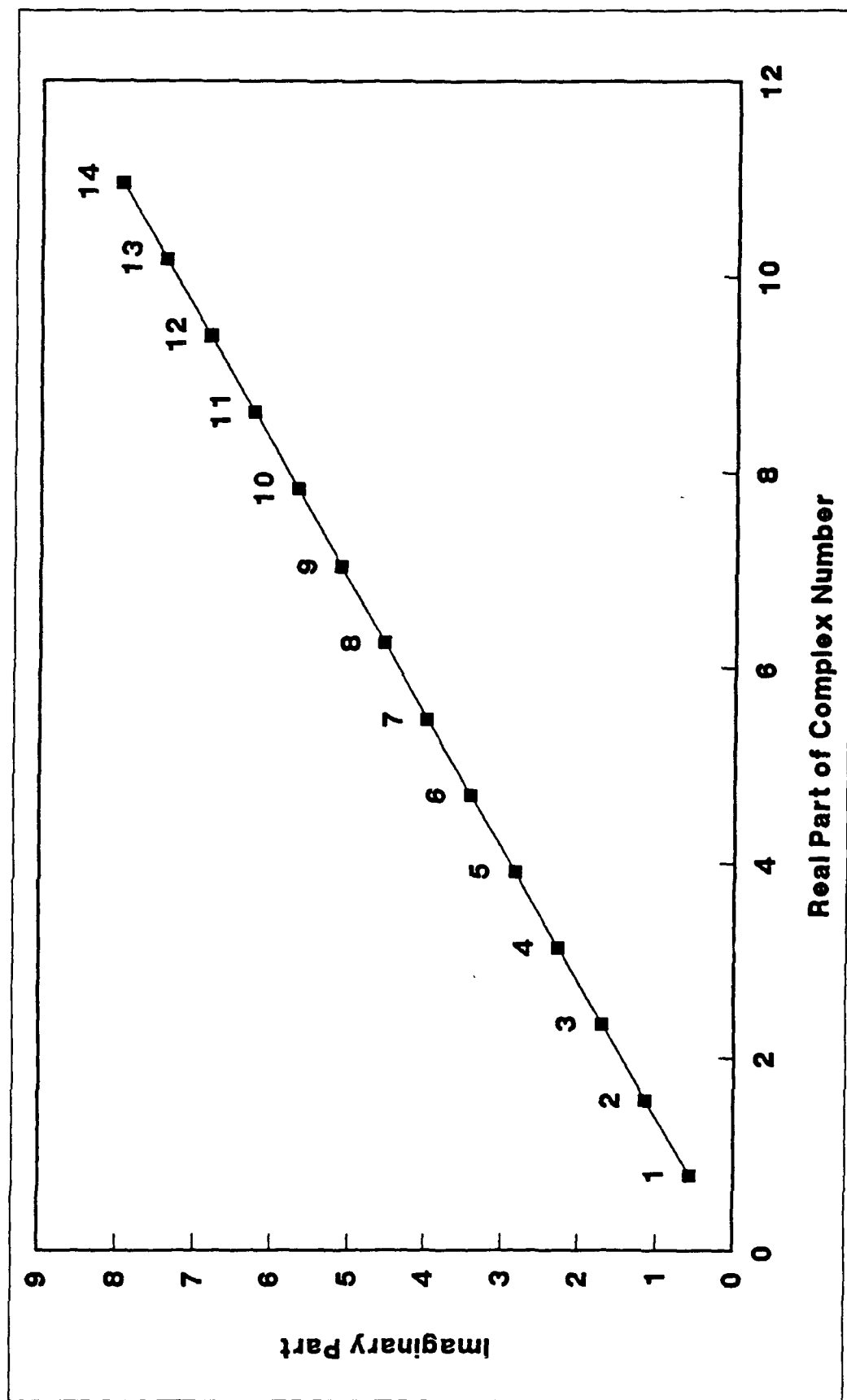
Figure 8. The 19-Hz cumulative sum of CSD (input is a 19.1-Hz cosine wave). Point 7 represents the sum of the CSDs from [0,1] : [1,2] up to [6,7] ; [7,8]
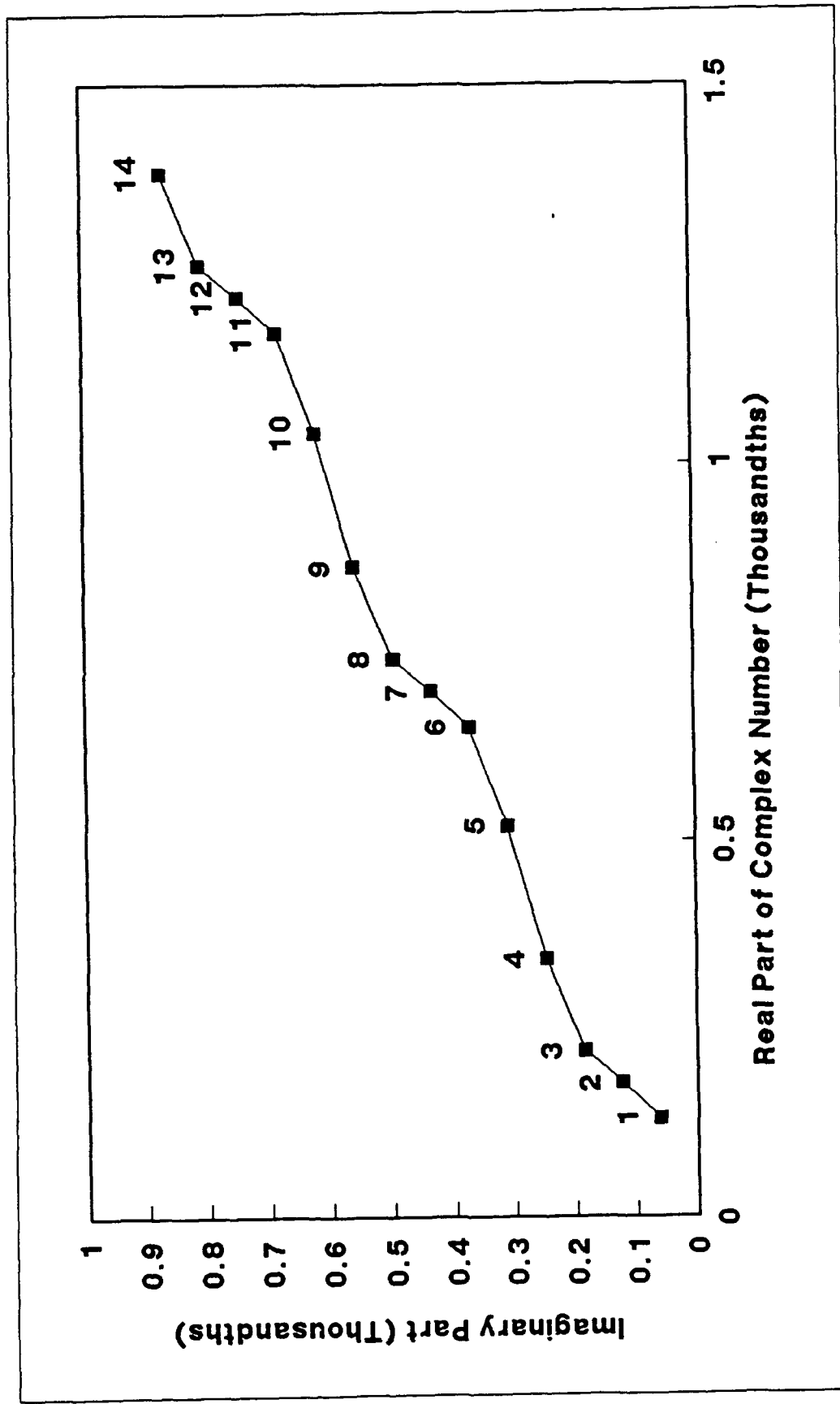
Figure 9. The 10-Hz cumulative sum of CSD (input is a 19.1-Hz cosine wave). Point 7 represents the sum of the CSDs from [0,1] : [1,2] up to [6,7] : [7,8]. The coherence is 0.881 for this frequency
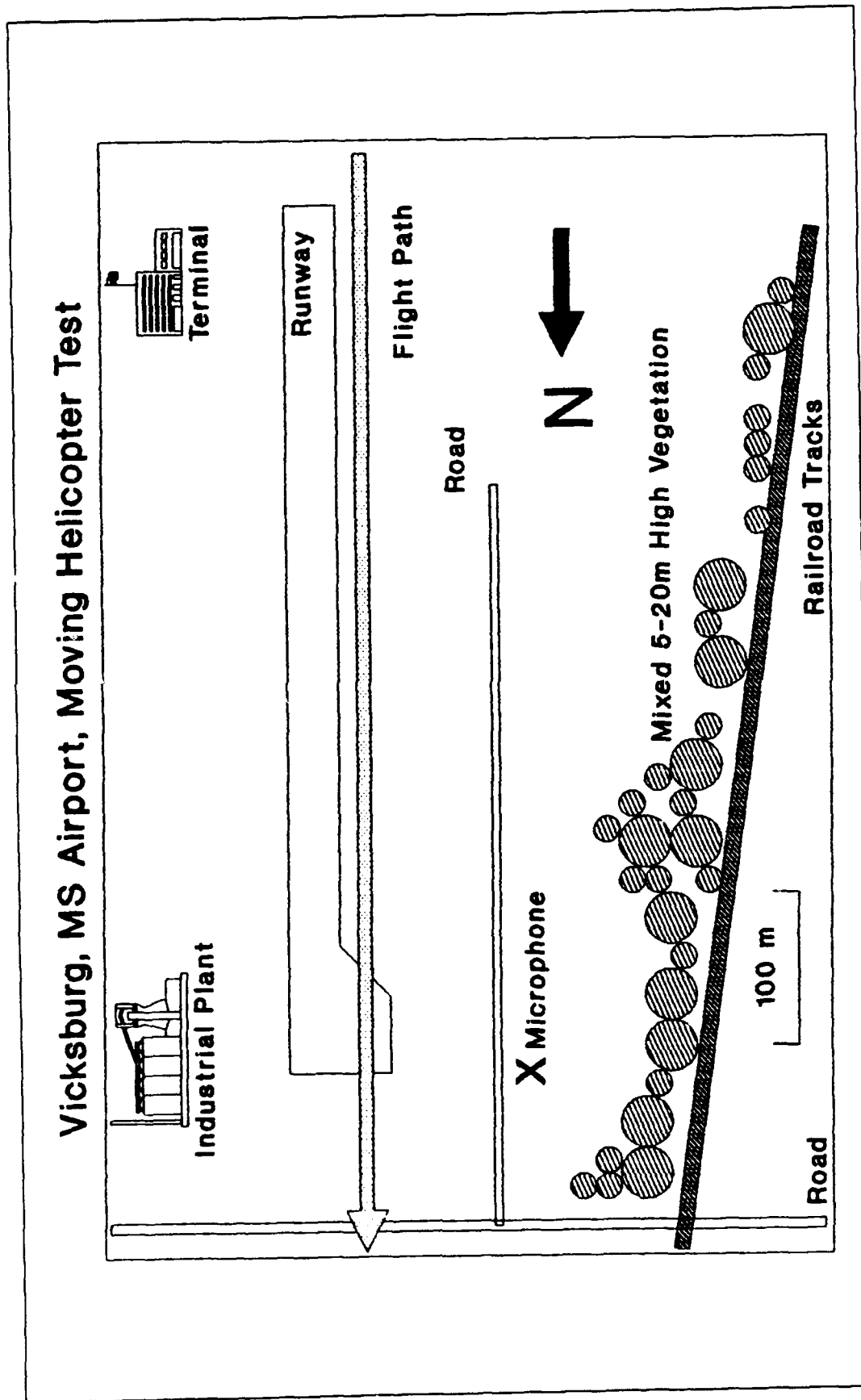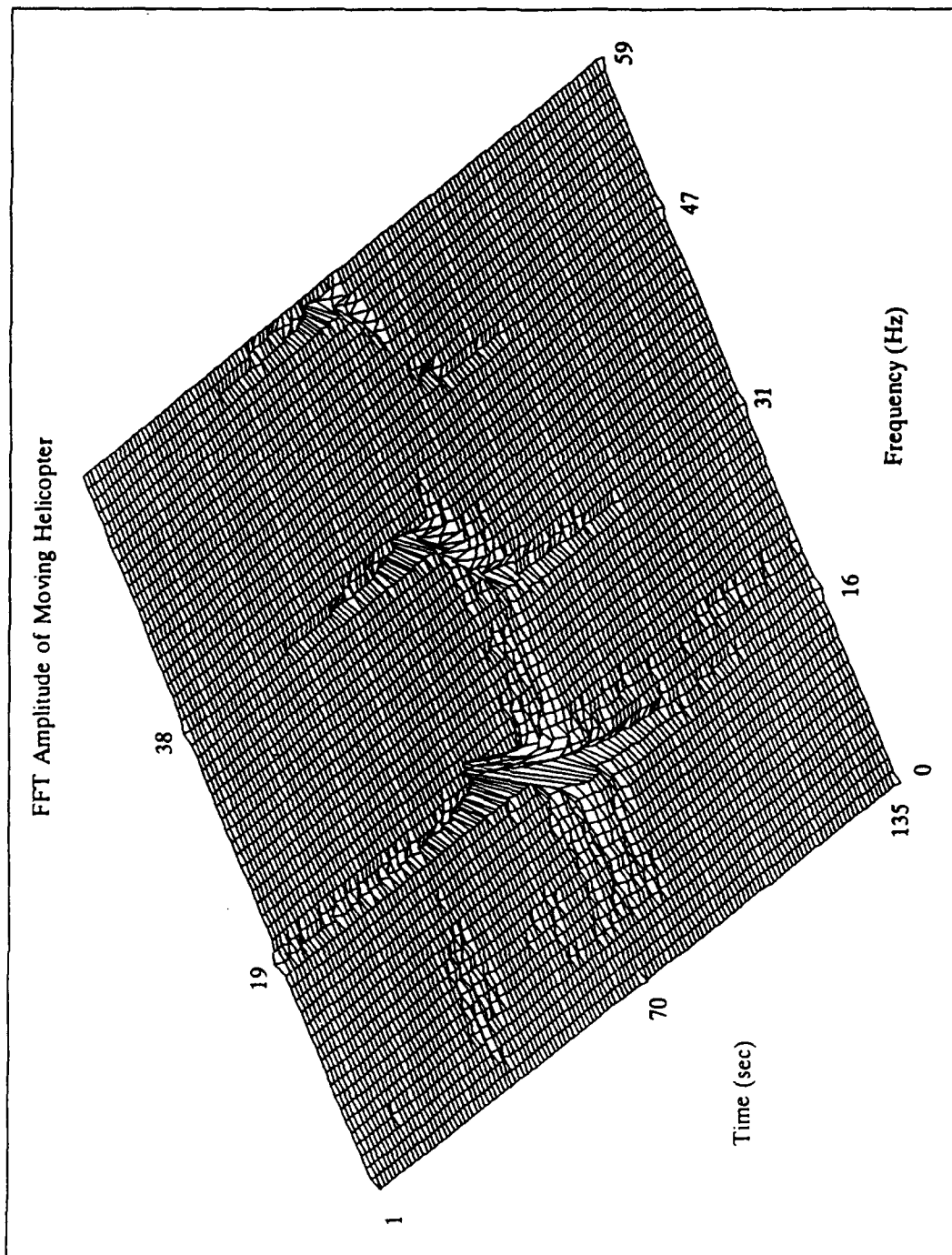
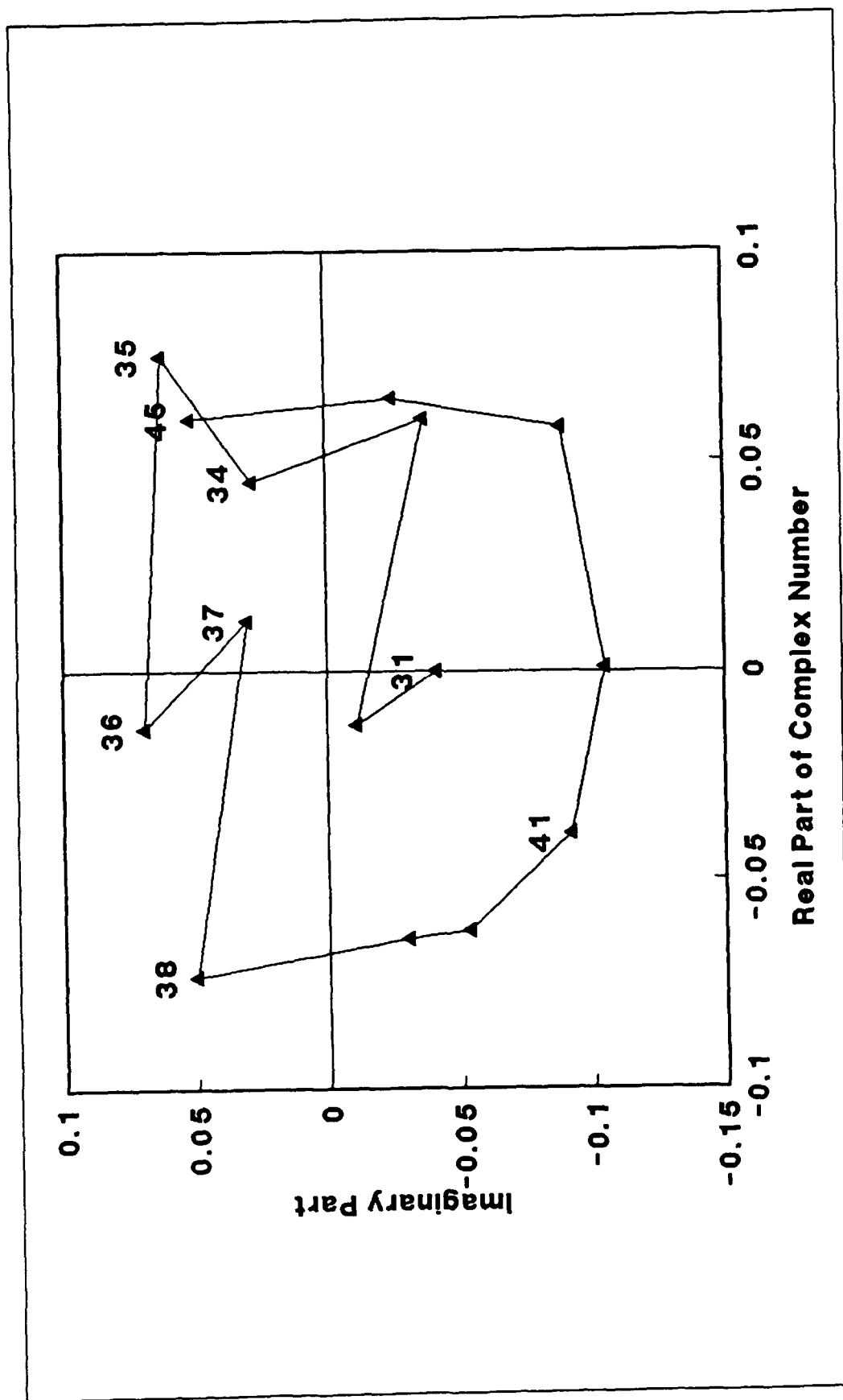Figure 10. Field geometry

FFT Amplitude of Moving Helicopter

Time (sec)

Frequency (Hz)

Figure 11. FFT analysis of a moving helicopter

Figure 12. FFT analysis of temporal coherence of 19-Hz energy of approaching helicopter during the time interval [30,45]. The coherence was 0.700 for this total time period of Run 21. The label represents the ending time of the 1-sec-long FFT interval
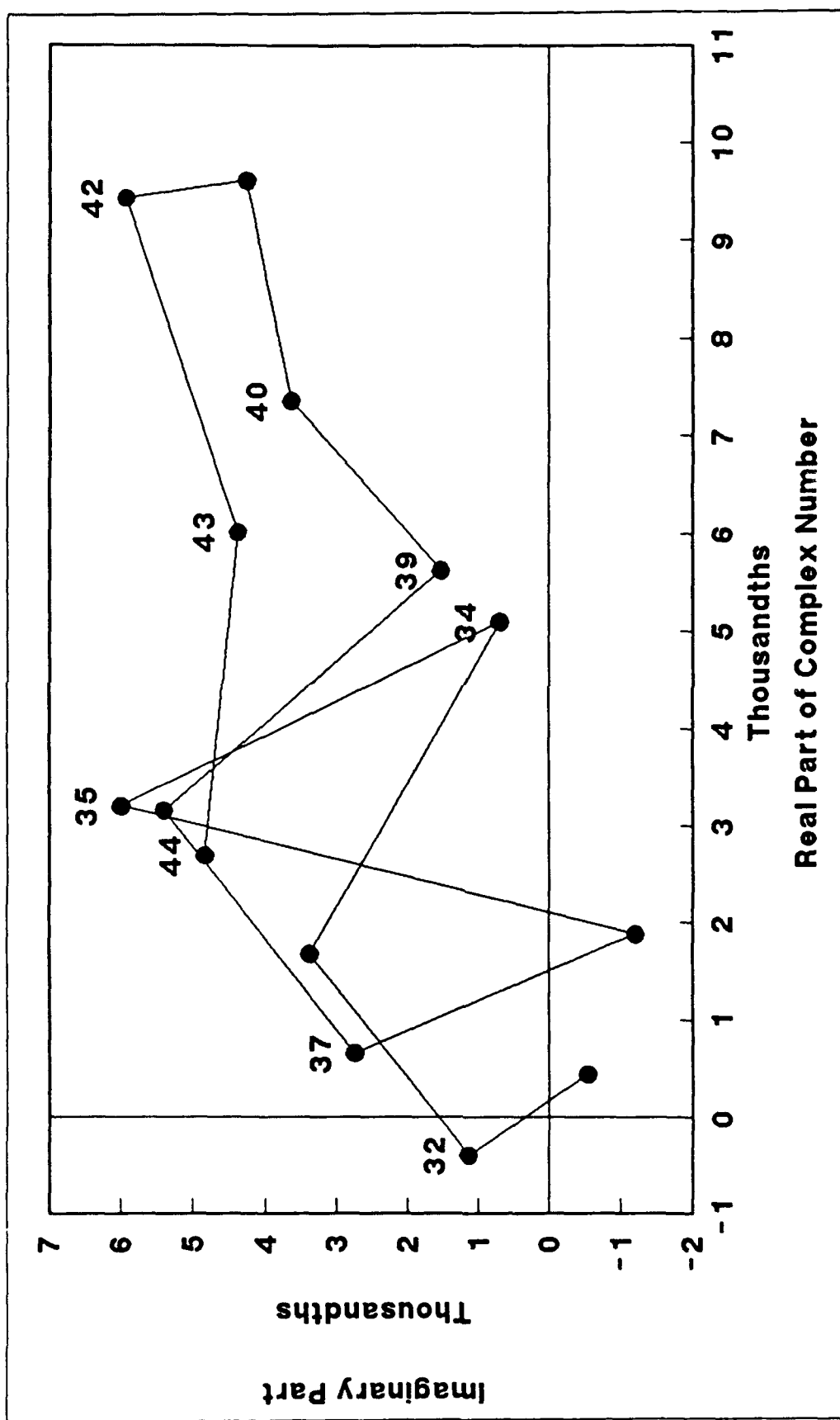
Figure 13. Cross-spectral density analysis (19 Hz, approaching helicopter, Run 21). The point labeled 42 is the CSD comparison of the FFTs of the interval [41,42] : [42,43] and is an estimate of the 19-Hz signal at 42 sec
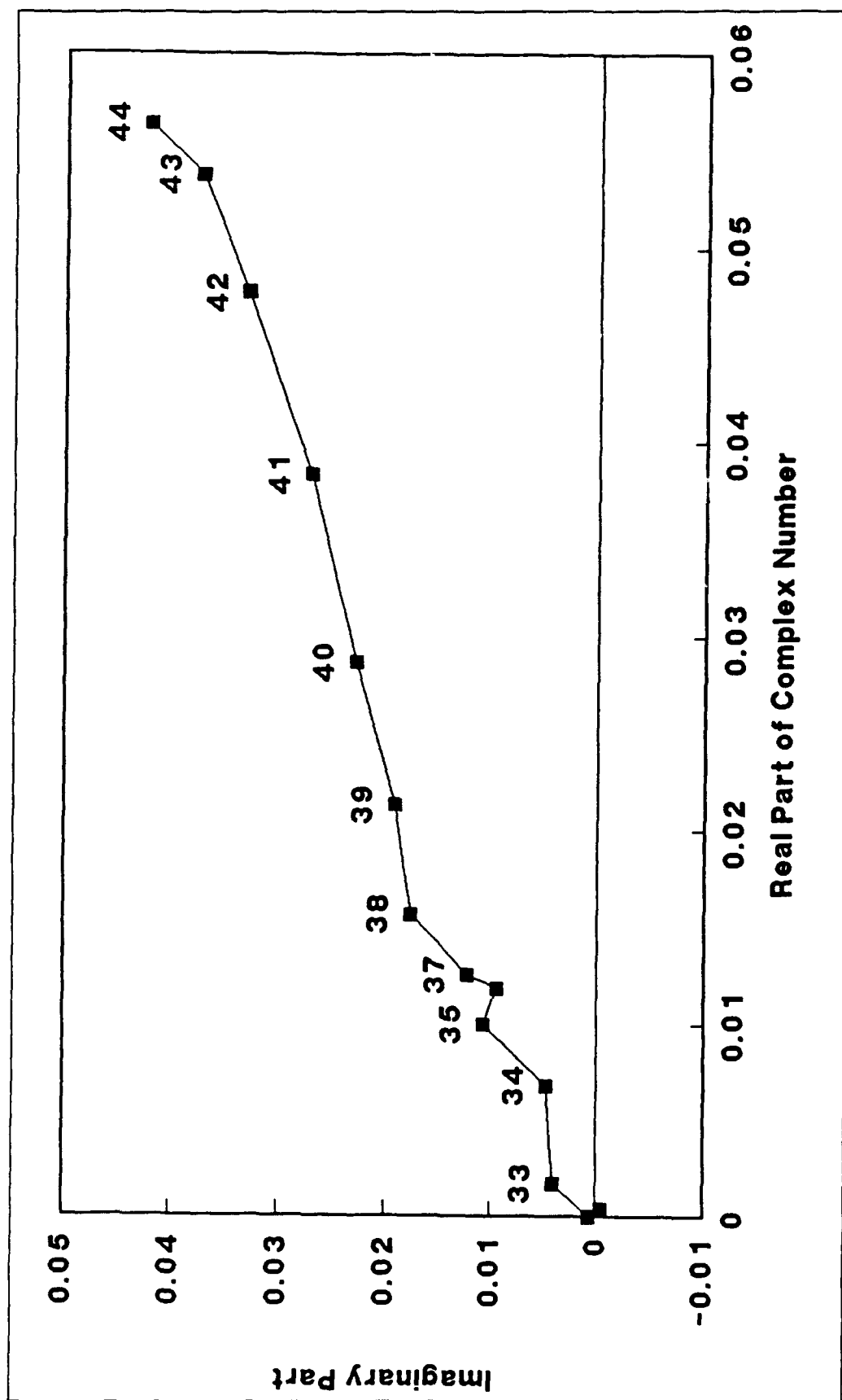
Figure 14. Cumulative sum of CSD (19 Hz, approaching helicopter, Run 21). The point labeled 42 is the sum of the 12 complex CSD numbers that compare [30,31] : [31,32] all the way up to [41,42] : [42,43]
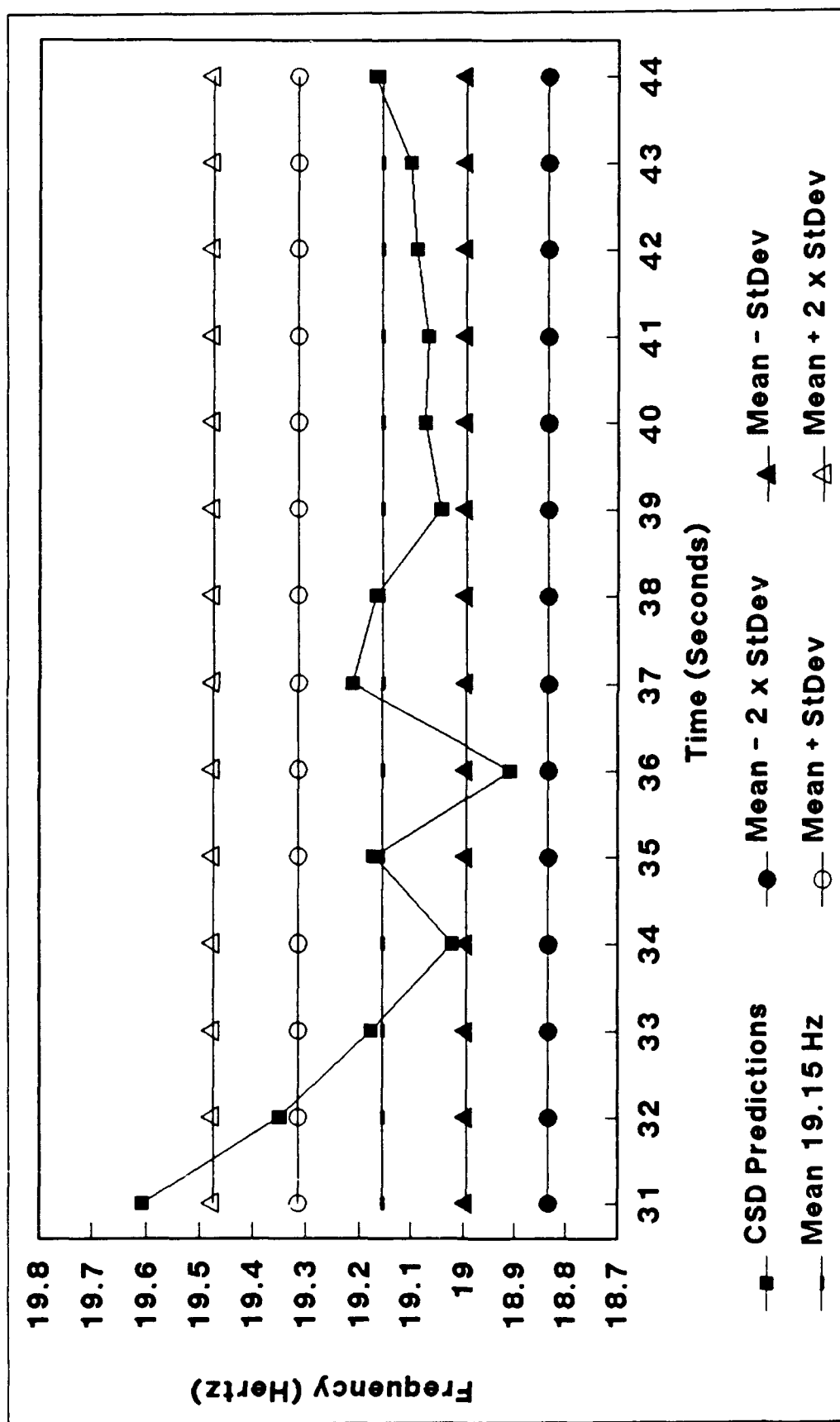
Figure 15. Frequency predicted by individual cross-spectral densities of approaching main rotor energy, Run 21, channel 1.
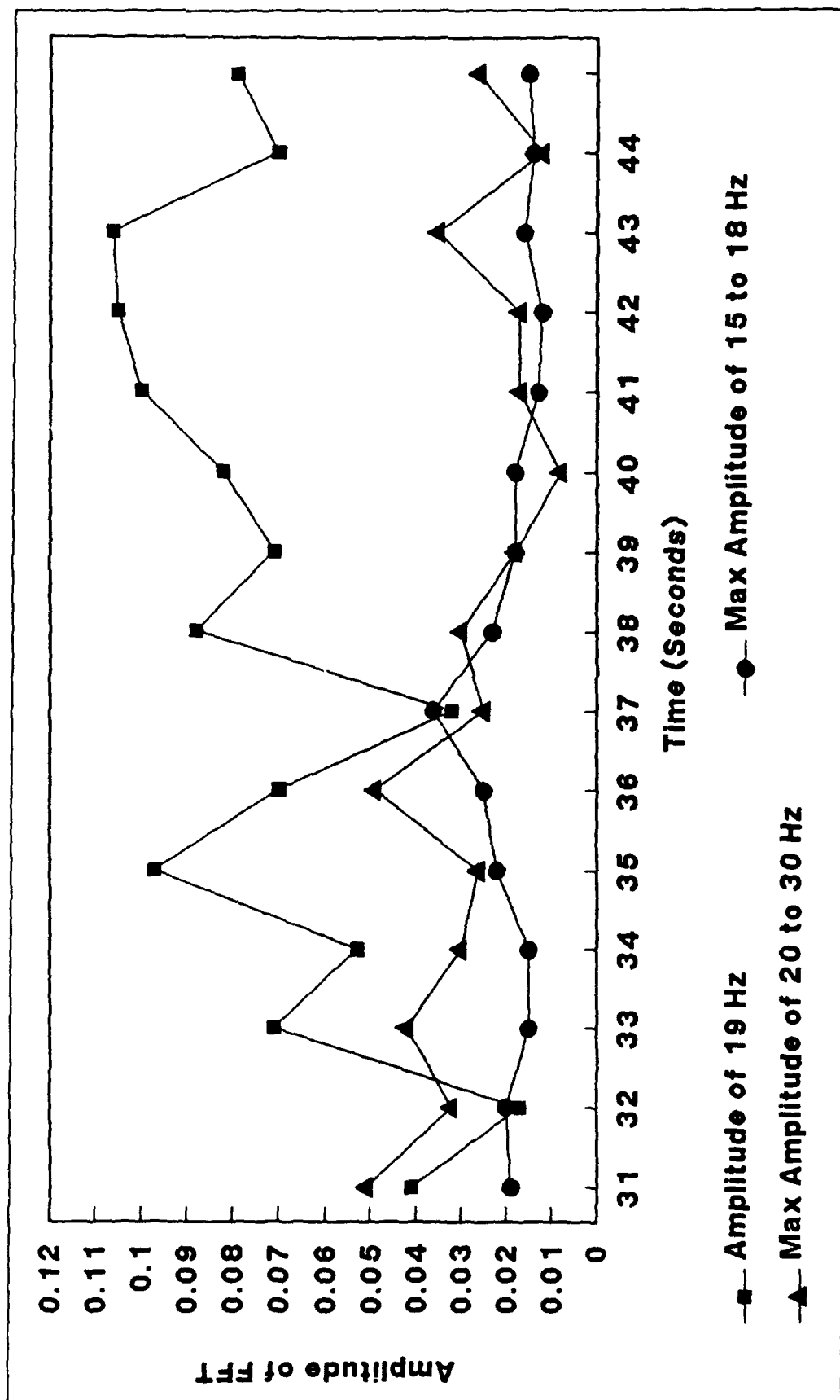Note: the standard deviation (StDev) is 0.16 Hz

Figure 16. Comparison of amplitudes of FFT of approaching 19-Hz energy, Run 21, channel 1 where velocity = 33 m/sec, altitude = 152 m, horizontal offset = 100 m (perpendicular offset = 182 m). The time is the end of the 1-sec-long interval
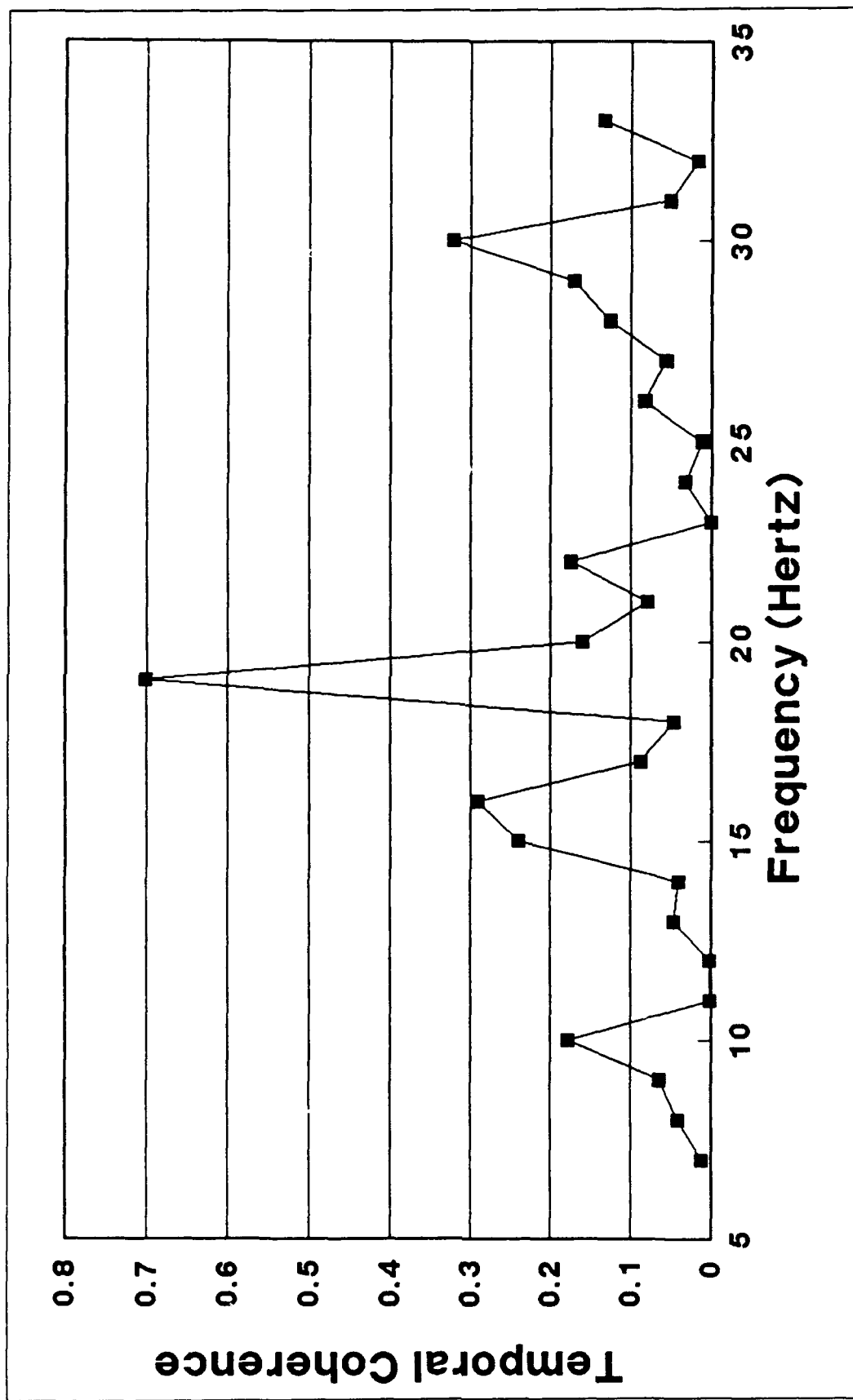
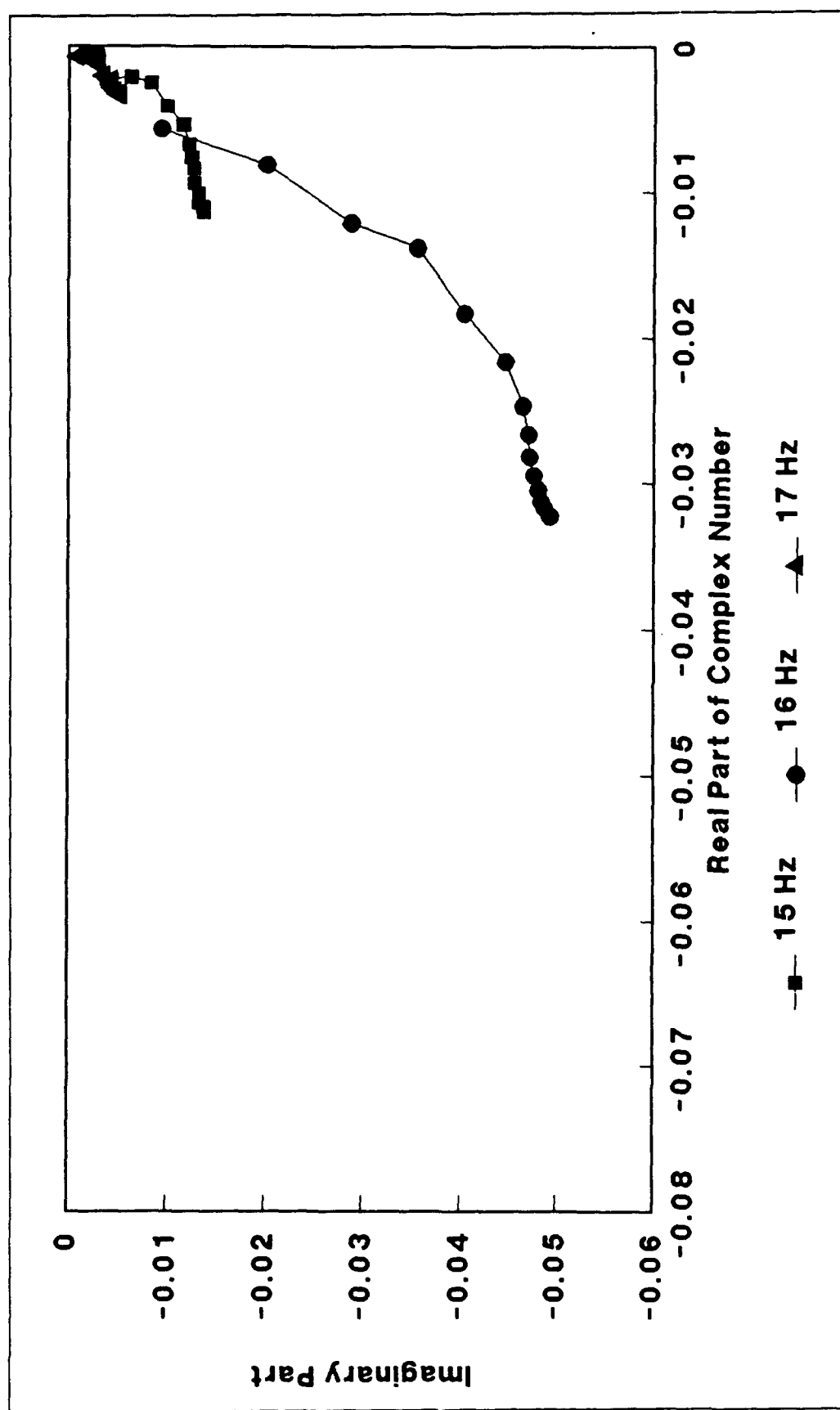Figure 17. Coherence over [30,45] of far-field approaching energy, Run 21, channel 1 moving helicopter

Figure 18. Cumulative sum of CSD for retreating helicopter of frequencies 15, 16, and 17 Hz with coherences 0.717, 0.877, and 0.712 over time [90,105] - Run 21, Vicksburg Airport, June 21, 1990
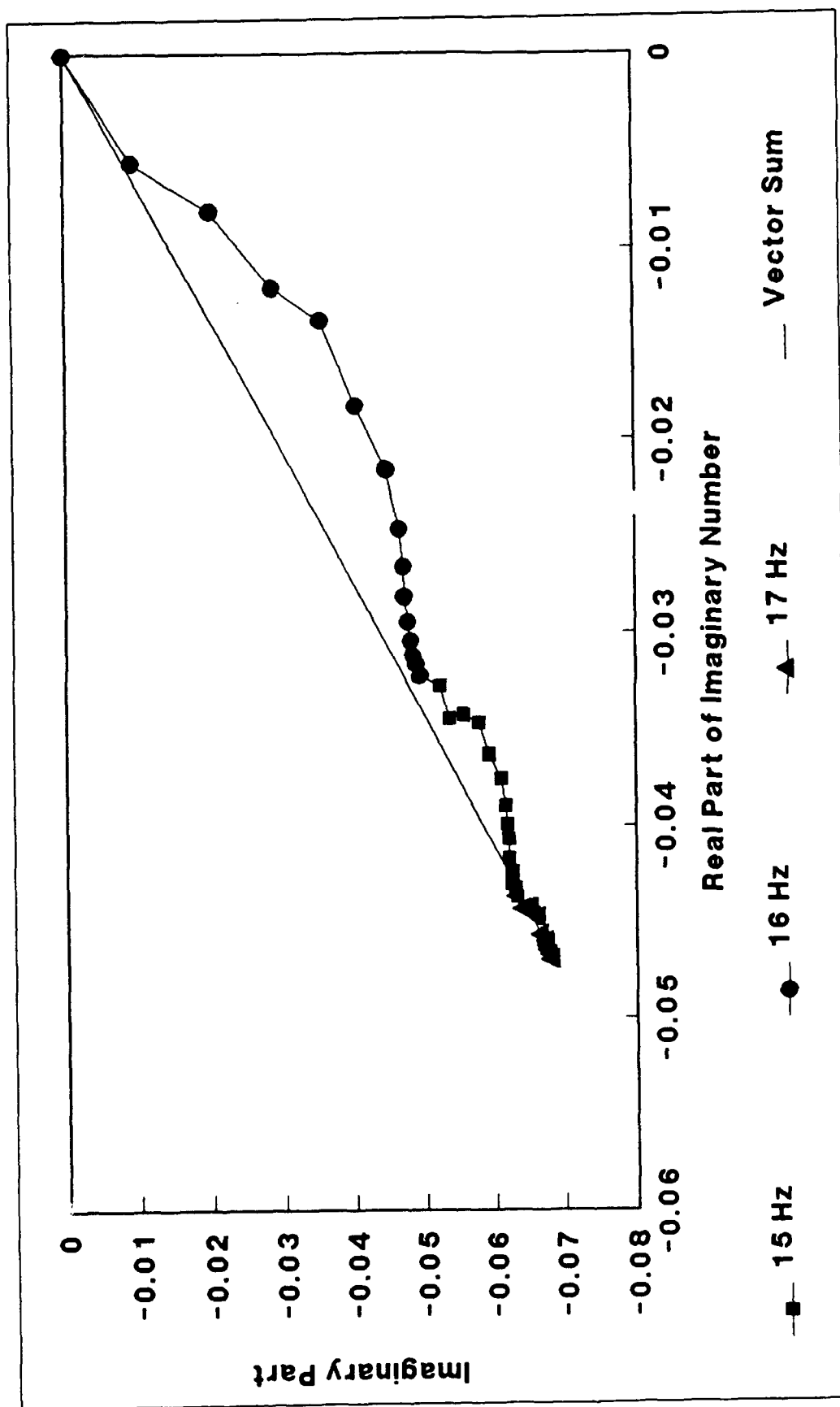
Figure 19. CSD sum of all coherent energy of main rotor blades for retreating helicopter of frequencies 15, 16, and 17 Hz with coherences 0.717, 0.877, and 0.712 over time interval [90,105]. Angle -0.35 cycle from positive real axis, implies frequency 15.65 Hz

Figure 20. Frequency predicted by cross-spectral density of the main rotor blades' energy crossing CPA, Run 21, channel 1

Figure 21. Prediction of range at CPA utilizing the slope of Doppler shift, Run 21, channel 1. The pilot-reported range includes the 0.52-sec shift from CPA to receiver

Appendix A
Definitions

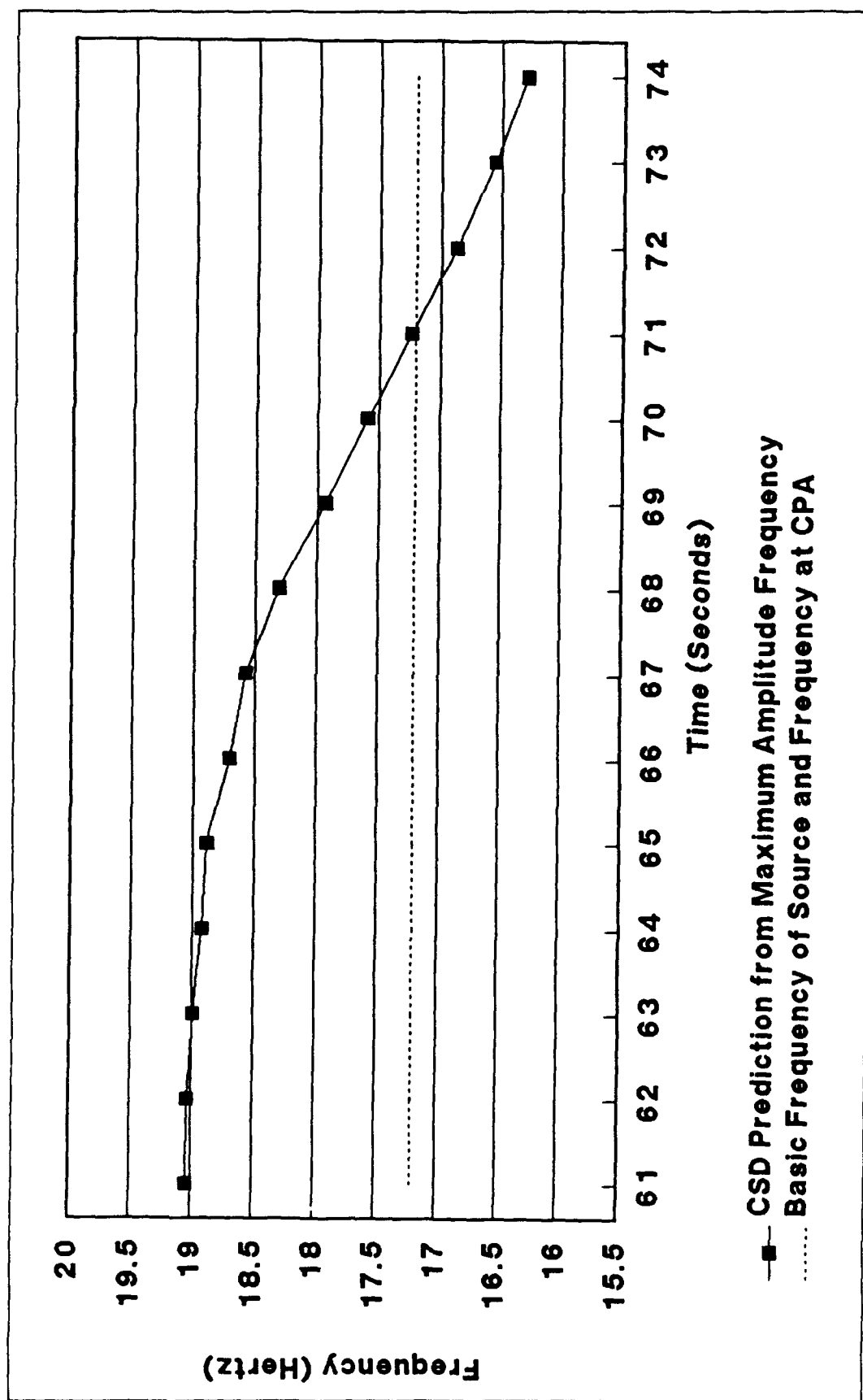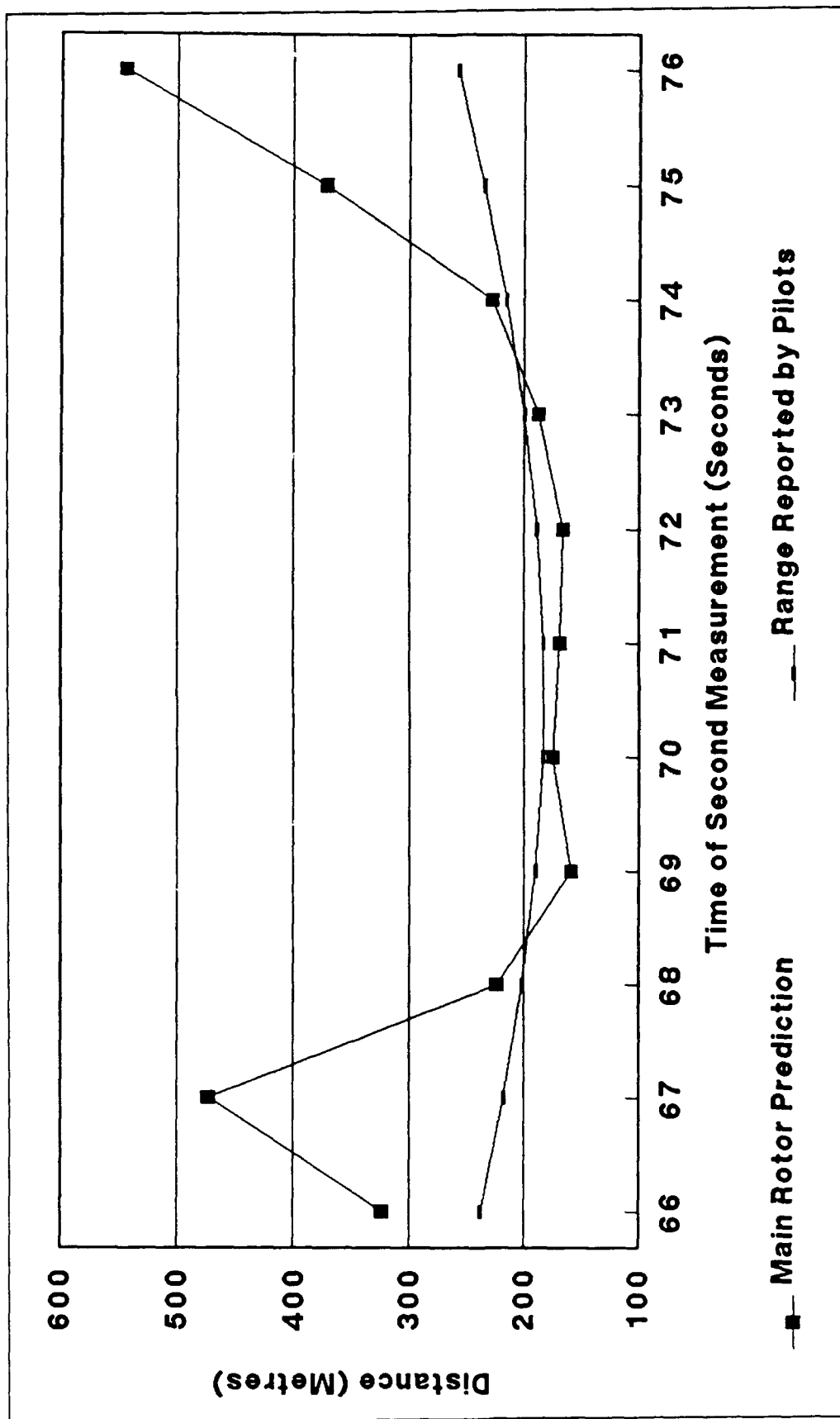| Term	Description
Alias	The process by which a continuous analog high frequency f (above the Nyquist frequency f_n) signal appears to look like a lower frequency f_a after digitally sampling at discrete times, as determined by the formula: $f_a = Minimum \mid f - k \cdot 2 \cdot f_n \mid$ where the minimum is computed over all positive integers k.
Basic frequency	Any isolated band of frequency energy that has not been Doppler shifted (e.g., fundamental of main rotor blades, second harmonic of main rotor blades, third harmonic of main rotor blades, fundamental of tail rotor blades, ...)
Frequency bin	The discrete number that the Fast Fourier Transform (FFT) assigns to each frequency of a real input signal. For example, a 1-sec-long 19.1-Hz signal would have most of its energy assigned to the 19-Hz FFT bin with the second largest amount of energy assigned to the 20-Hz FFT bin.
Fundamental frequency	The lowest frequency of a periodic function.
Harmonic	A frequency which is an integer multiple of a fundamental frequency. The second harmonic, for example, has a frequency twice that of the fundamental.
Nyquist frequency	The maximum frequency f_n that can be accurately recorded digitally at a particular sampling rate dt in time: $F_n = \dfrac{1}{2 \cdot dt}$
Periodic function	A function that repeats after a specific interval of time.

Appendix B
Clarification of Various Frequencies

This report mentions many different types of frequency measurements and variables. The key to understanding is to realize the precise type of frequency that is under discussion at each stage. This appendix attempts to clarify these concepts as they relate to physics (i.e., acoustics) and applied mathematics and computing (i.e., signal processing).

Table B1 separates the frequencies into four categories. The first category represents the mechanical revolution rate. The second category applies to those frequencies that can be acoustically detected at the source. This category includes the prominent mechanical frequencies and harmonics. Any frequency in this second category is considered a "basic frequency" in this document. There are some major changes in the frequencies from where the sound is generated to where it is recorded at some stationary receiver on the ground. The third category describes how the acoustic signal is sensed at the microphone on the ground. Such frequencies are usually referred as "Doppler- shifted frequencies" in the text. The final category represents a leap into the mathematical world of the standard computational tool, the Fast Fourier Transform (FFT), that is used to analyze measured signals of amplitude as a function of time. This world, "the frequency domain," reports all of its measurements in terms of frequencies: hence it takes more work in that domain to detect and analyze the acoustical frequencies that can be measured at the receiver.

Mechanical Frequencies

The mechanical frequencies are those that are most easily understood by the layman. They are the frequency of revolution of physical moving parts of a machine. Hence, they can be seen and readily comprehended. For a helicopter (see Table B2) they include the revolution rate of the rotor shafts and engine. The blades also represent a revolution rate that is the product of the shaft revolution rate times the number of blades on that shaft. This formula assumes that the blades are all designed alike and are spaced an equal distance around the shaft.

Acoustically Generated Frequencies at Source

Although there are many mechanical frequencies on the helicopter, not all of them generate significant acoustic signal. The blades generate much more noise than the shafts. For the purpose of this report the shafts do not appear to generate any measurable signal and will not be considered as an acoustically generated frequency. The blade frequencies are acoustically measurable, however (see Table B3).

If the acoustical signal generated by one set of blades appears to be a perfect sine wave, then reporting that frequency is sufficient. In most cases the wave does not appear to be a perfect sine wave. Higher harmonics (see Appendix A) are present in the acoustical signal. Normally, each higher harmonic has a lower amplitude than its predecessor.

Any acoustically generated frequency at the source is synonymous with the term "basic frequency." As documented in the Doppler theory section of Chapter 2 of this report, if the basic frequency is known and not changing over time, then accurate knowledge of the Doppler-shifted frequency recorded at a microphone fixed on the ground as the helicopter is approaching permits the determination of the velocity and range at the closest point of approach (CPA) of a helicopter traveling at a constant velocity in a straight line. If the basic frequency is not known, it can be determined through the knowledge of the Doppler-shifted frequency at the microphone using all time (both approaching and retreating).

The basic frequencies are measured at the source (also referred to as "the helicopter point of view"). They should also be sensed by a microphone that is close to the helicopter when neither helicopter nor microphone is moving and there is no wind.

Acoustically Measured Frequencies at Receiver

At the normal receiver (e.g., a microphone) the recorded signal has been changed from those generated at the source. When the source is moving relative to the receiver and there is no wind, a Doppler shift in the frequency occurs:

$$f(t) = f_o \cdot \frac{1}{1 - \frac{V(t)}{C}} \tag{1}$$

where

$f(t)$ = Doppler-shifted frequency at time t

f_o = basic frequency

$V(t)$ = velocity that the source is approaching the receiver at time t

C = velocity of sound

Figure 1 in the main text illustrates how the Doppler-shifted frequency compares to the basic frequency. As the source is approaching the receiver, $V(t) > 0$ and the Doppler-shifted frequency is higher than the basic frequency. At CPA, $V(t) = 0$ and they are both equal. As the helicopter is going away from the microphone, the Doppler-shifted frequency is less than the basic frequency. The microphone senses the Doppler-shifted frequency, not the basic frequency.

Some additional changes are seen in the recorded signal: first, the amplitude of the entire signal is decreased in proportion to the distance the sound traveled from the source to the receiver. Second, the amplitude of the higher frequencies are normally diminished more than the lower frequencies because of the attenuation of the atmosphere. The addition of background noise near the receiver prevents the detection of weak signals from the source. Finally, the microphone itself often introduces some distortion to the signal due to a phase change and minimum amplitude cutoff caused by transforming the pressure wave in the air into an electrical response in the microphone. This imposes some analog frequency filtering (often to avoid aliasing the signal), finally transforming the analog signal into a digital signal.

FFT Mathematical Output of Computer

The FFT is an algorithm that decomposes an input signal reported as an amplitude at equal time increments (referred to as the "time domain") into both an amplitude and phase at equal increments of frequency ("frequency domain"). The transformation assigns the largest amplitudes in the frequency domain to those frequencies that are most evident in the time domain.

The discrete FFT is defined as follows: given amplitudes g_k recorded at time t_k where

$$t_k = t_o + k \cdot \delta t \tag{2}$$

and

$$k = 1, 2, ..., 2^n,$$

then the FFT defines a complex number $F(f_j)$ at each real frequency f_j

$$f_j = j \cdot \delta f \qquad j = 0, 1, 2, ..., 2^{n-1}, \tag{3}$$

where the frequency increment f is defined as

$$\delta f = \frac{1}{2^n \cdot \delta t} \tag{4}$$

and $F(f_j)$ is defined by the formula

$$F(f_j) = \delta t \cdot \sum_{k=1}^{2^n} g_k \cdot \exp(2\pi i \cdot t_k \cdot f_j) \tag{5}$$

The amplitude $A(f_j)$ and phase (f_j) are defined as real numbers in the normal complex variable sense (Ahlfors 1966) so that

$$F(f_j) = A(f_j) \cdot \exp[2\pi i \cdot \theta(f_j)] \tag{6}$$

The amplitude represents the strength or amount of that frequency f_j present in the time domain signal. The phase represents the time delay or shift from a cosine wave of that frequency.

The last frequency f_j, where $j=2^{n-1}$, is called the Nyquist frequency. It is important that all coherent energy for frequencies larger than the Nyquist be removed before computing the FFT. Otherwise, that energy will be reported incorrectly by the FFT as some energy less than the Nyquist. This incorrect reporting is called "aliasing."

All of the amplitudes and phases are considered to apply to the time interval over which the summation occurred: $[t_0, t_0+2^n \cdot \delta t]$. This frequency analysis can easily be repeated for later time intervals. Figure 11 in the main text shows the amplitudes of the FFT analysis of the measured data for the first sixty frequencies (at a 1-Hz increment) and for one hundred and thirty-five 1-sec-long time intervals. That graph contains three bands of Doppler-shifted energy: the fundamental of the main rotor blades (basic frequency at 17.2 Hz, approaching at 19 Hz and retreating at 16 Hz), the second harmonic of the main rotor blades (basic frequency at 34.4 Hz, approaching at 38 Hz and retreating at 31 Hz), and the third harmonic of the main rotor blades (basic frequency at 51.6 Hz, approaching at 57 Hz and retreating at 47 Hz). The decrease in amplitude at the higher harmonics is quite evident.

The tabular representations of parts of Figure 11 in the main text are shown in Tables 5, 8, and 11 (again in the main text). The corresponding phase information appears in Tables 6, 9, and 11 in the main text. The prominent energy of the fundamental energy appears as the frequencies with large amplitudes in the frequency domain that can be tracked from one time interval to the next (i.e., the bold numbers).

The main restriction of the FFT is the restriction that the discrete steps δf forces on the frequency resolution of the energy band. The main purpose of the Accurate Calculation of Frequency section of Chapter 2 of this report (pp 10-11) is to obtain an improved accuracy over the normal FFT

resolution. This higher resolution was necessary for the formula for the range at CPA calculated using the Doppler theory of physics.

Table B1 Description of Different Frequency Values
Mechanical
■   Rate of revolution of moving parts
Acoustically Generated at Source (i.e., basic frequencies)
■   Restrict mechanical frequencies to those that are audible
■   Add the higher harmonics (see Appendix A)
Acoustically Measured at Receiver
■   Add Doppler shift to acoustically generated frequencies
■   Decrease amplitude due to distance traveled
■   Impose minimum detectable amplitude due to
■   Limits of measuring device
■   Background noise exterior to measuring device
FFT Mathematical Output of Computer
■   Report amplitude and phase at equal increments of frequency for any signal recorded at equal time increments
■   Impose FFT limitations
■   Frequency starts at 0 Hz
■   Frequency increment is inverse of total time interval analyzed
■   Maximum frequency reported is Nyquist frequency
■   Frequencies higher than the Nyquist that are present in the input time signal are incorrectly reported as frequencies below the Nyquist in the frequency domain

Table B2
Example of Mechanical Frequency Rates for Helicopters

- Main rotor shaft revolution rate r_1
  (e.g., 4.3 Hz)

- Main rotor blades revolution rate
  r_2 = (# blades on main rotor shaft) * r_1
  (e.g., 17.2 Hz = 4 * 4.3 Hz)

- Tail rotor shaft revolution rate r_3
  (e.g., 19.8 Hz)

- Tail rotor blades revolution rate
  r_4 = (# blades on tail rotor shaft) * r_3
  (e.g., 79.2 Hz = 4 * 19.8 Hz)

- Turbine engine shaft revolution rate r_5
  (e.g., 300 Hz)

- Turbine engine blades revolution rate
  r_6 = (# blades on turbine engine shaft) * r_5
  (e.g., 3,000 Hz = 10 * 300 Hz)

Table B3
Example of Acoustically Generated Frequency Rates for Helicopter Sources

Components:

- Main rotor blades and all harmonics
  f_{1k} = k * r_2 for k = 1, 2, 3, . . .
  (e.g., 17.2 Hz, 34.4 Hz, 51.6 Hz, 68.8 Hz, 86.0 Hz, . . .)

- Tail rotor blades revolution rate
  f_{2k} = k * r_4 for k = 1, 2, 3, . . .
  (e.g., 79.2 Hz, 158.4 Hz, 227.6 Hz, . . .)

- Turbine engine blades revolution rate
  f_{3k} = k * r_6 for k = 1, 2, 3, . . .
  (e.g., 3,000 Hz, 6,000 Hz, 9,000 Hz, . . .)

Composite Results:

Sequence of isolated bands of energy at discrete frequencies (Hz): 17.2, 34.4, 51.6,
68.8, 79.2, 86.0, 103.2, 120.4, 137.6, 154.8, 158.4, 172.0, 189.2, . . .

Appendix C
Additional Statistics of Other Signals

All real data possess some noise that causes problems with well-intentioned algorithms. The acoustic data of Run 21 (Figure 11 in the main text) is no exception. Fortunately, signals other than the fundamental of the main rotor can be used to estimate some of the information concerning the helicopter. Both the second harmonic (approaching at approximately 38 Hz) and the tail rotor (at roughly 80 Hz) can be tracked long enough to make some of these measurements.

These are essentially independent measurements of the velocity, range, and the time of the closest point of approach (CPA). The variations of the separate statistics hint at the magnitude of the error in the calculation. Since the input data to the calculations are real, the output data represent the accuracy of both the algorithm and its sensitivity to recording and digitizing noise. Results of the frequency calculations are listed below in Table C1. The velocity calculation for all three energy packages is very similar (see Table C2). All three cross-spectral density (CSD)-derived velocities are above the velocity reported by the pilot and below the velocity predicted by the Global Positioning System (GPS). The CSD

Table C1 Summary of Frequency Analysis, All Three Strong Signals			
Acoustic Predictions	Main Rotor		Tail Rotor
	Main Frequency	2nd Harmonic	
Approaching frequency (Hz)	19.10	38.20	88.09
Retreating frequency (Hz)	15.65	31.26	72.20
Basic Frequency (Hz)	17.21	34.38	79.36
Known frequencies (Hz)	17.2	34.4	79.3

**Table C2
Summary of Velocity, Time, & Range at CPA, All Three Strong Signals**

Acoustic Predictions	Main Rotor		Tail Rotor	Pilots Reported	GPS Estimates
	Main Frequency	2nd Harm			
Velocity (m/sec)	34.98	35.20	34.95	33.46	35.95[1]
Time of CPA (sec)	71.07	71.39	71.40	61[2]	[3]
Range at CPA (m)	167	166	141	182	169

[1] Approach velocity average of time intervals [15,45] & [90,105].
[2] Includes 1.5-sec addition for the helicopter moving from opposite between Arrays A and B to opposite Array A and 0.5 sec for the sound to travel from the helicopter to the receiver.
[3] There was no independent correlation of digitizing time to GPS time.

velocities must therefore be considered accurate within the level of accuracy for the independent measurements of the pilot's report and the GPS.

Ranges predicted at various times for all three signals consistently indicate a number slightly below that reported by the pilots (see Figure C1). The CSD range predictions agree well with the estimate of the GPS system.
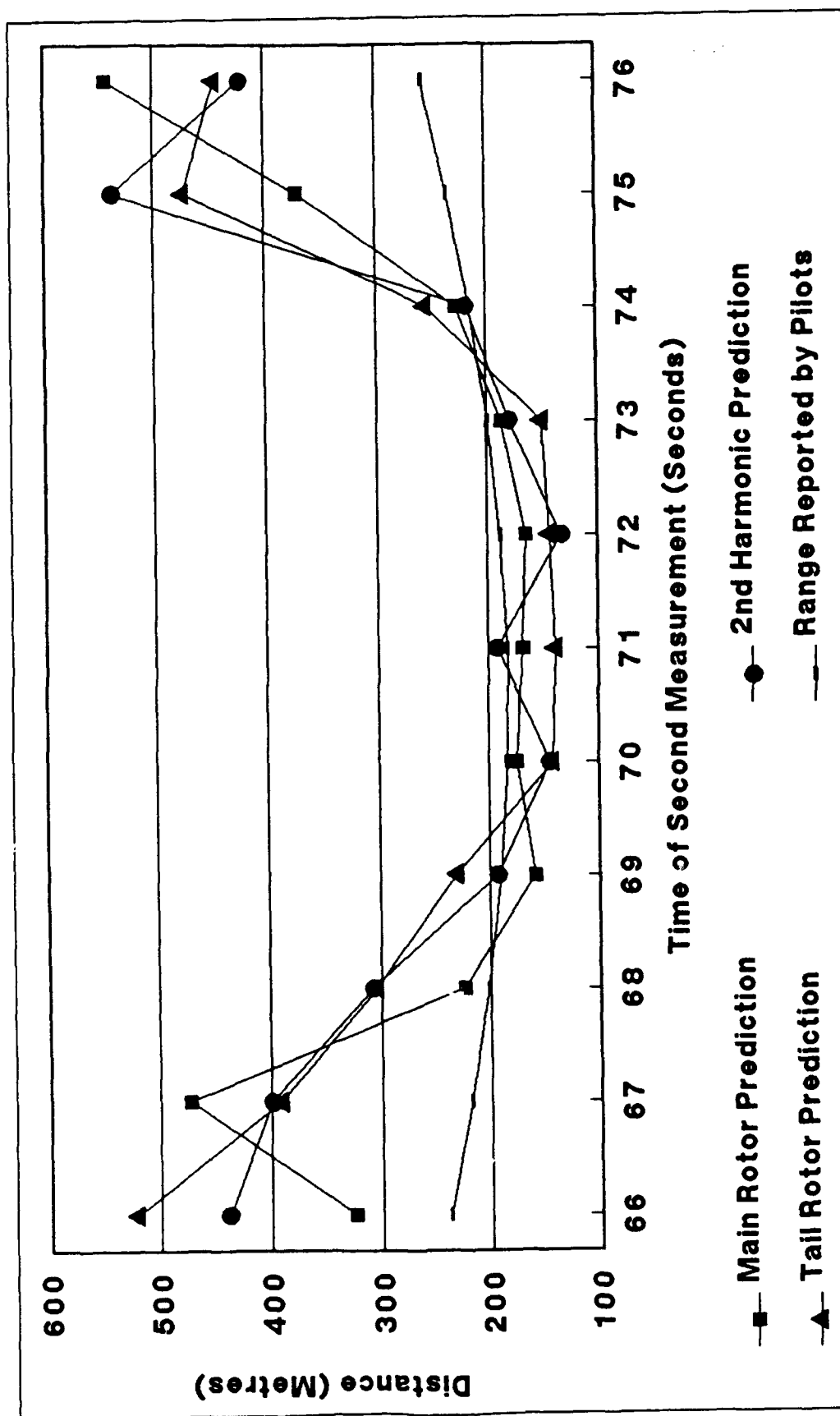
Figure C1. Best three signals' prediction of range at CPA utilizing the slope of Doppler shift - Run 21 - channel 1. Total perpendicular offset = 182 m. The pilot-reported range includes the 0.52-sec shift from CPA to receiver

Appendix D
Notation

A	Amplitude
C	Velocity of sound, m/sec
CPA	Closest point of approach
CSD	Cross-spectral density
$f(t)$	Frequency measured at receiver at time t, Hz
f_a	Far-field approaching frequency, Hz
f_o	Basic acoustic frequency, Hz
f_r	Far-field retreating frequency, Hz
FFT	Fast Fourier Transform
$g(t)$	Fourier approximation of h(t) at one frequency
GPS	Global Positioning System
$h(t)$	Simulation of an acoustic amplitude at time t
$H_n(f)$	FFT over [n,n+1] of the signal h(t) at f hertz
i	Complex imaginary unit $(-1)^{1/2}$
t	Time, sec
t_{CPA}	The time the helicopter was at CPA, sec
$t_{CPA}(t)$	Estimate made at time t of t_{CPA}, sec
t_o	Time when the ground is receiving sound of CPA, sec

$t_o(t)$	Estimate made at time t of t_o, sec
R	Range at CPA, distance of helicopter to microphone, m
$R(t)$	Estimate made at time t of the range at CPA, m
TemCoh(f)	Temporal coherence of signal at the frequency f
V	Velocity of the source, m/sec
WAM	Wide-Area Mine
X	Point in the complex number plane
$X_n(f)$	The CSD of $H_n(f)$
θ	Phase, degrees, radians, or cycles
β	Phase difference, degrees, radians, or cycles
δf	Frequency increment, Hz
$|z|$	Amplitude of the complex number z
$*$	Complex conjugate operator

D2